Influence of biomass co-firing on SCR catalyst deactivation

Marcin Adam Kiełtyka

Thesis to obtain the Master of Science Degree in

Energy Engineering and Management

Supervisors: Prof. Ana Paula Vieira Soares Pereira Dias

Prof. Teresa Grzybek

MSc. Eng. Henryk Kubiczek

MSc. Eng. Bartosz Sarapata

Examination Committee

Chairperson: Prof. José Alberto Caiado Falcão de Campos

Supervisor: Prof. Ana Paula Vieira Soares Pereira Dias

Members of the Committee: Prof. João Fernando Pereira Gomes

Prof. Mário Manuel Gonçalves da Costa

February 2015

Acknowledgments

This thesis is based on work conducted within the KIC InnoEnergy Master School, in the MSc program Clean Coal Technologies. This program is supported financially by the KIC InnoEnergy. The author also received financial support from KIC InnoEnergy, which is gratefully acknowledged.

KIC InnoEnergy is a company supported by the European Institute of Innovation and Technology (EIT), and has the mission of delivering commercial products and services, new businesses, innovators and entrepreneurs in the field of sustainable energy through the integration of higher education, research, entrepreneurs and business companies. Shareholders in KIC InnoEnergy are leading industries, research centers, universities and business schools from across Europe.

http://www.kic-innoenergy.com

The MSc program Clean Coal Technologies is a collaboration of:

AGH University of Science and Technology, Kraków, Poland,

SUT Silesian University of Technology, Gliwice, Poland

IST Instituto Superior Técnico, Universidade de Lisboa, Portugal

This work was realized under the agreement on cooperation between R&D department of EDF Polska, which provided samples to analyse, as well as information regarding the power plant operation.

Summary

SCR catalyst from a coal-fired power plant (Poland) was characterized in order to identify the deactivation processes. The received monoliths of $DeNO_X$ catalyst, with yellow-light green shades, were TiO_2 supported V_2O_5 catalyst modified with tungsten oxide (V_2O_5-WO_X/TiO_2). Four samples with different operation times (fresh, 3, 6 and 12 months) showing a maximum deactivation of 25% (approximately) were characterized in order to identify the deactivation processes. The received catalyst monoliths showed partial plugging of channels with fly ashes (cenospheres). This process can be partially responsible for the activity decay since part of the catalyst bed become unavailable. The elemental analysis performed for fresh and post reaction catalyst, by AAS and EDS during SEM, showed deposition of alkali elements (Na, K, Ca) which promotes a decrease of the surface acidity evaluated by 1-butene to 2-butene isomerization. The UV-Vis spectra showed only minor changes on the vanadium oxidation state whereas XRD remains unchangeable for all the analyzed catalysts. The physical-chemical characterization of the fresh and post reaction catalysts seem to point out the alkali deposition as the main deactivation process for the SCR studied catalyst.

Keywords: NOx, static sources, SCR catalysts, V_2O_5-WOx/TiO_2, deactivation, fly ashes, alkali deposition

Resumo

Para a identificação dos processos de desactivação em catalisadores de remoção de NO_X caracterizaram-se amostras provenientes duma central termoeléctrica, Polaca, a carvão. Os monólitos recebidos, com cor amarelo-esverdeado clara, foram identificados como catalisadores de pentóxido de vanádio (modificado com óxido de tungsténio) suportados em titânia. As quatro amostras com diferentes tempos de operação (fresco, 3, 6, 9 e 12 meses) apresentavam uma desactivação máxima de 25%. Os monólitos recebidos apresentavam parte dos canais bloqueados por cinzas volantes (cenoesferas). Este processo pode ser responsável por parte da perda de actividade catalítica uma vez que uma fracção do catalisador fica inacessível aos reagentes. A análise química das amostras de catalisador fresco e após reacção, por AA e EDE durante MEV, mostrou a deposição de elementos alcalinos que promove a diminuição da acidez determinada por isomerização do 1-buteno a 2-buteno. Os espectros de UV-Vis mostraram diferenças insignificantes para o estado de oxidação das espécies de vanádio nas amostras com diferentes tempos de reacção. Os difractogramas de raios X de todas as amostras não mostraram diferenças, correspondendo maioritariamente ao material de suporte do catalisador (TiO_2). A caracterização físico-química das amostras de catalisador, com diferentes tempos de reacção, parece apontar a deposição de elementos alcalinos como o maior responsável pelo processo de desactivação.

Palavras-chave: NOx, carvão, catalisadores DeNOx, V_2O_5-WOx/TiO_2,desactivação,cinzas volantes, deposição de elementos alcalinos

Thanks

I would like to thank all the people who helped me during preparation of this thesis, as well as those, who supported me in writing. In particular I would like to thank:

Prof. Teresa Grzybek, for all the help, knowledge and time spend, even on holidays with the most professional approach, that allowed me to have a glimpse how scientific work look like,

Prof. Ana Paula Soares Dias, for all the time spend making experimental part of this thesis possible and for guiding me through IST,

MSc. Henryk Kubiczek, for cooperation and help in acquiring the samples for tests as well as for providing all needed information about them,

MSc. Bartosz Sarapata, for cooperation and help in acquiring the samples for tests as well as for providing all needed information about them,

MSc. Rafał Baran, for help in measurements and advising in experimental part preparation,

MSc. Dorota Makowska, for help in measurements,

My family, friends and girlfriend for help and support.

Table of contents

Index of figures

Index of tables

Index of abbreviations

SCR – Selective Catalytic Reduction

SNCR – selective non catalytic reduction

BAT – Best Available Technique

AAS – Atomic Absorption Spectrometry

XRD – X-ray Diffraction

EDS – Electron Dispersive Spectroscopy

λ – Air excess coefficient [-] or X-ray wavelength [pm]

A – absorbance[-]

k – absorbance coefficient [dm3 /cm*g]

c – concentration of measured element in absorbing layer [g/dm3]

l – thickness of the absorbing layer [cm]

n – diffraction order, small integer

d – distance between atomic layers

Θ – angle between radiation beam and the normal to sample surface

IR – infrared

η – conversion in 1-butene isomerization reaction[-]

∆x – relative loss of activity

x – conversion in SCR reaction

R – determination coefficient

1. Introduction

Electric energy is one of the most desirable goods in modern world. Many techniques have been developed for its production but a majority of power plants are still based on fossil fuels combustion. Among gas, oil and coal, the solid fuels have the biggest share in electric energy production. Lignite and hard coal combustion units are highly developed nowadays, the modern ones operating at >40% of overall efficiency. Even with sophisticated technology there are still drawbacks, mostly caused by the fuel used. The most important one is environmental impact of coal-based power plants.

Heat produced in coal combustion is the most desirable effect of fuel oxidation. It is accompanied by transforming coal, including its moisture and mineral matter attached, into exhaust gases, bottom ash and fly ash. Each has to be treated in a proper way to minimize the impacts on the environment. Exhaust gases are responsible for air pollution problem. Most dangerous are SO_2 and NO_x. They are only a small fraction of entire exhaust gases volume, but taking into account huge amounts of flue gases released by every power plant a year, they are becoming a significant threat to be dealt with. This is the reason why European Union Commission is setting the emission limits to both of those gases, as well as other pollutants being by-products of combustion process. There are two important documents that point how modern power plant should operate. First one is European Commission Directives, which sets emission limits for every specified production unit, depending on size and type of fuel used. The most recent Directive connected to power plants is 2010/75/UE. Second one are Best Available Techniques (BAT), which is proposing techniques needed to achieve limits described in the first one. One of the means for decreasing NO_x emissions is selective catalytic reduction (SCR), using ammonia and a catalyst to convert nitrogen oxides to elemental nitrogen and water. It was proven to be the most efficient post combustion method, and it is used in many units around the world with success.

Apart from NO_x and SO_2, carbon dioxide, one of by-products causing great concern, as it is one of the greenhouse gases, molecules that may lead to climatic changes. Despite the fact that there are many natural sources of CO_2, it has been stated that the rising levels of carbon dioxide in the atmosphere are to a great extend influenced by the combustion of fossil fuels, including coal. Coal and lignite have the biggest share in CO_2 formation per unit of electricity produced from their combustion. One way of reducing carbon dioxide emissions is to use biomass as a part of the fuel mixture. It has been proven that it is possible to co-fire coal with biomass in powerplants without major retrofits, even if biomass has worse combustion properties than traditional fuels. This work aims to study the influence of biomass co-combustion on the performance and deactivation of commercial DeNOx catalyst used in a full scale boiler of the existing power plant.

2. Techniques of NOx emission reduction

NOx is a mixture of nitrogen and oxygen compounds: nitric oxide (NO) and nitrogen dioxide (NO_2). There are three mechanisms of NOx formation during combustion, depending on the origin of nitrogen. Thermal NOx formation results from the reaction between oxygen and nitrogen from air. High temperature is required for this reaction to occur. Fuel NOx are formed from nitrogen compounds present in the fuel used. The last group, prompt NOx, are formed by the conversion of molecular nitrogen in the flame front in the presence of intermediate hydrocarbon compounds. The amount of NOx created by prompt mechanism is much smaller than by the two other reactions. As the formation of thermal NOx depends on temperature, at combustion process carried out below 1000^oC, most emissions come from fuel nitrogen. The amount of NOx produced by fuel mechanism is the largest in coal fired power plants, with higher emission from brown coal than from hard coal.

There are two groups of techniques used to reduce NOx emissions. Primary methods are concentrated on reducing NOx formation rate during combustion. It is achieved by changing conditions inside the boiler, such as flame temperature, amount of oxygen and combustion volume. Primary methods are considered to be cheaper than secondary ones, but they offer lower reduction efficiency. Secondary methods use chemical reaction to reduce already created NOx. They use a reducing agent in quantities depending on the boiler power, and thus the running costs of a power plant can significantly increase. This group of methods is considered more expensive but it grants higher efficiency.

2.1 Primary methods

There are several types of primary methods:

- low excess air
- air staging
- flue gas recirculation
- reduced air preheating
- fuel staging
- low NOx burners

2.1.1 Low excess air

Low excess air is an operational way for lowering the emission of nitrogen oxides. By decreasing the amount of oxygen in the combustion area to the minimum value compulsory for complete combustion, fuel bound nitrogen conversion and thermal NOx formation are reduced. It is

due to lower temperature and less nitrogen than in case of excess air. A significant emission reduction can be achieved by this method, especially in the case of old power plants, and this is the reason why it was implemented in many existing large power plants. In general, new plants are equipped with extensive measuring and control devices that enable the adjustment of the combustion air supply to the optimum value.

Unfortunately lowering the amount of oxygen can result in incomplete combustion which leads to the decrease of steam temperature, high carbon monoxide emission, reduction in boiler efficiency and even slagging and corrosion. It implicates several safety problems including fires in air preheaters and ash hoppers when used without strict control system. The efficiency of this method can vary between 10-44%. The advantages of this method are: no additional energy is required, no reduction in the availability of the power plant is registered and the method is comparatively easy to implement. The disadvantages are: combustion may become incomplete, the amount of unburned carbon in ash may increase and it can lead to high levels of carbon monoxide in flue gases.

2.1.2 Air staging

Air staging method is based on the concept of creating two combustion zones. The primary zone with sub-stoichiometric oxygen content (90-70%of stoichiometric value) reduces conversion of bonded nitrogen and also suppresses the formation of thermal NOx due to lower temperature during combustion. The secondary zone is supplied with additional 10-30% of combustion air to complete the oxidation process. Low temperature in the secondary zone results in the decrease of the rate of thermal NOx formation. Overall NOx emission reduction efficiency of this technique is between 10-70%. There are three options of applying air staging method in boilers:

- biased burner firing – only for vertical boilers, with lower burners operating at fuel-rich mixture and upper burners being supplied with excess air,
- burners out of service (BOOS) – this method does not require any major changes in combustion installation. Lower burners operate at fuel-rich mixture when upper burners supply only air, and
- overfire air – requires the installation of additional air boxes above the top row of burners. This leads to burners operating at low excess of air. Overfire air ensure complete combustion. This method also requires modifications of water-wall to provide space for extra air nozzles.

The advantages of this method are: it is an inexpensive way of lowering NOx emissions, it does not increase energy consumption of the power plant and it does not have any adverse effects on its operational availability if properly applied. The disadvantages are: a significant amount of CO may

be formed if the air nozzles are not well situated and the amount of unburned carbon may increase in the case of retrofit.

2.1.3 Flue-gas recirculation

Flue-gas recirculation method uses a part of exhaust gases to lower the amount of oxygen in the combustion zone, thus decreasing temperature. It results simultaneously in the reduction of conversion of fuel nitrogen and the decreased formation of thermal nitrogen oxides [Kuropka, 1991]. This method has proven to be effective in the reduction of NOx emissions in high flame temperature systems. In coal-fired power plants emission reduction can only reach ca. 20% but in gas-fired plants its efficiency can reach 50%, when flue-gas recirculation is combined with overfire air method. [Kordylewski & Hardy, 2000]

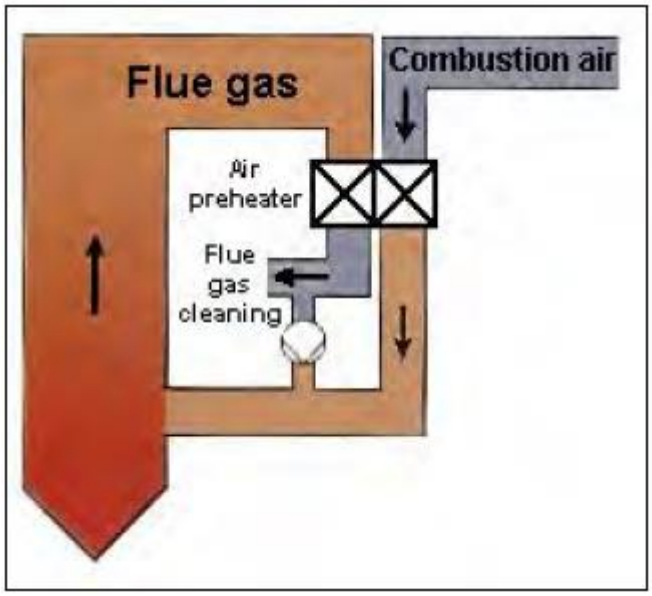

Figure 1 Schematic representation of flue gas recirculation [European Commission, 2006]

Figure 1 schematically illustrates the flue gas recirculating method. Around 20-30% of flue-gas is taken from the main stream at temperature of 350-400^{o}C and injected back to the combustion zone. However, the method requires that flue gas is cleaned out of particulates, and additionally it requires the application of special burners design. The amount of recirculated flue-gas should not exceed 30 %, or otherwise, several problems, including corrosion and efficiency loss may occur.

2.1.4 Reduced air preheating

Air preheating uses thermal energy of exhaust gases to warm the combustion air. This technique is a common way of increasing thermal efficiency of power plant as a whole. The reduction

in air preheating leads to lower combustion temperature. This allows to achieve the reduction of the formation of thermal nitrogen oxides between 20-30%. [1]

2.1.5 Fuel staging

Fuel staging method is based on the concept of reducing already created nitrogen oxides to nitrogen. This is achieved by dividing the boiler into three zones:

- Primary combustion zone, where 80-85% of fuel is burned with almost stoichiometric oxygen level,
- Reburning zone, where secondary fuel is injected in the reducing atmosphere. At this stage fuel can be different from the primary one used, and
- The third zone, where excess air is added to combust the remaining fuel.

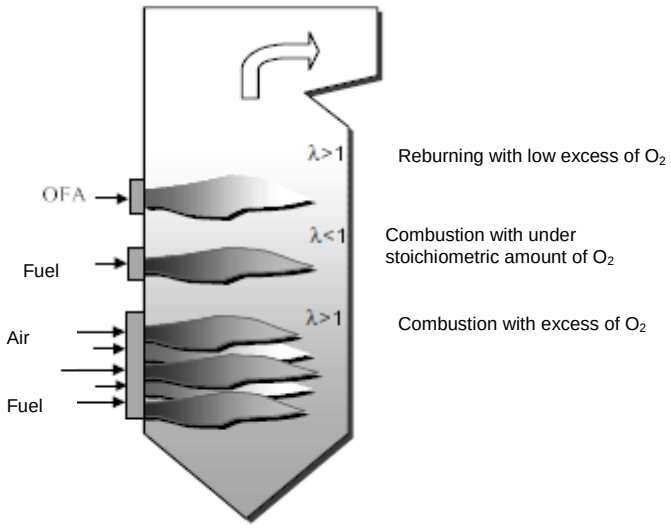

Figure 2 Schematic representation of fuel staging with overfire air boiler [Bulewicz et al. 2005]

Different fuels may be used as reburning agents. In case of pulverized coal or oil combustion in third stage, bound nitrogen present in structure of the fuel lead to NOx formation in the burnout zone. Using natural gas as secondary fuel enables to avoid this drawback. The efficiency of fuel staging method varies between 50-60% and depends on several aspects, such as:

- Temperature in the reburning zone should be as high as possible (1200^{o}C)
- Residence time in the combustion area should be between 0.4-1.5s
- Air stoichiometry in third stage should be in range of λ=0.7-0.9
- Air stoichiometry in primary zone should be around λ=1.1, and

- Fuel type used for reduction.

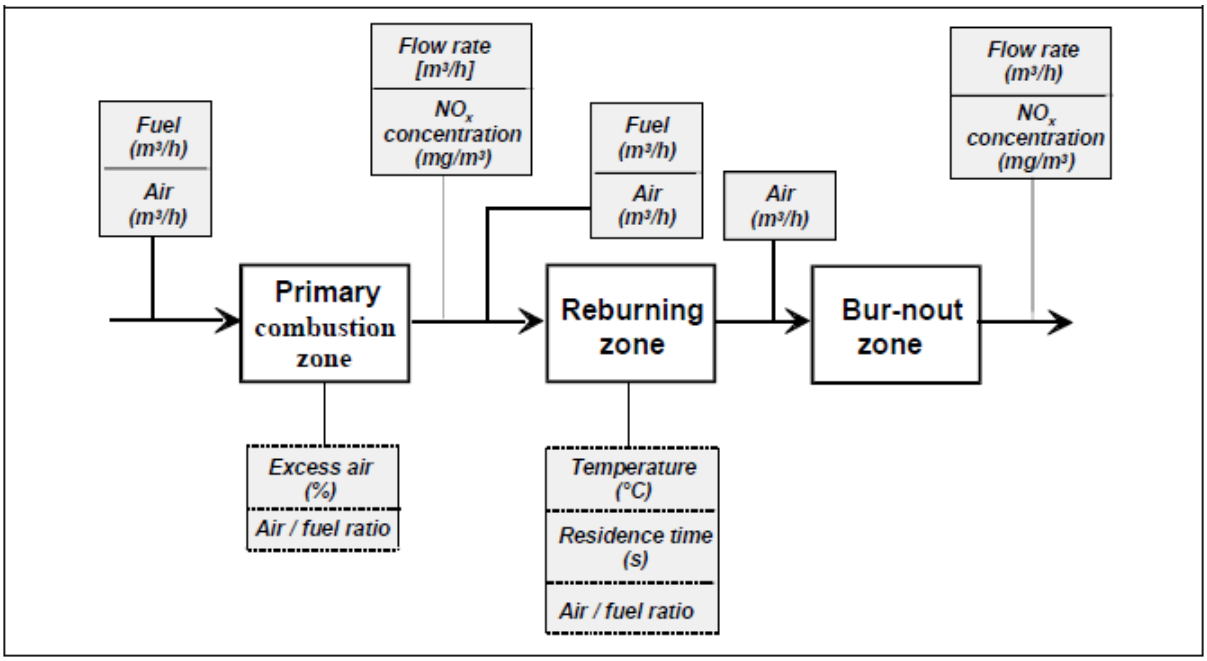

Figure 3 Schematic representation of fuel staging system

Figure 3 depicts fuel and air streams coming to different zones in the fuel staging method. This method can be implemented in all type of boilers. One of disadvantages is a larger combustion chamber volume required, which causes retrofitted power plants to have less power from a unit of boiler volume. Relatively high installation cost comparing to other methods is another drawback of fuel staging. [Kordylewski & Hardy, 2000]

2.1.6 Low NOx burner

Although low NO_x burners technology is well developed, research is still going on to improve the existing systems. A detailed design of each burner differs significantly depending on the manufacturer.

In a classical concept, air and fuel were mixed directly in the burner. This leads to the creation of flame with hot and oxidizing primary zone in the flame root and secondary colder zone at the flame end. Most of NOx are formed in the primary zone where temperature enables thermal oxidation of nitrogen from air. The influence of the secondary zone on the emission level is low.

Low NOx burners technique may lead to the decrease in NOx emissions by changing the way of the introduction of air and fuel into the flame. As a result from the delayed mixing of oxidant and the

combusted substance, the peak flame temperature is decreased, thus leading to the reduction in the formation of thermal NOx and bounded nitrogen conversion.

The application of this method requires to change the burners and the instalment of overfire air. It is almost always cost efficient if the previous boiler was equipped with classical burners. According to used technique low NOx burners can be divided into three groups:

- Air staged low NOx burner (25-35%) [Miller & Tillman, 2008]
- Flue gas recirculation low NOx burner (20%),
- Fuel staged low NOx burners (50-60%), and
- New generation of low NOX burners combining air-staging, fuel-staging and flue-gas recirculation.

1.2 Secondary methods

Two types of secondary methods may be considered for the reduction of NO_x from powerplants [Miller & Tillman, 2008, Bulewicz et al., 2005]:

- Selective non-catalytic reduction (SNCR)
- Selective catalytic reduction

1.2.1 Selective non-catalytic reduction (SNCR)

Figure 4 shows a schematic representation of SNCR method. The selective non-catalytic reduction (SNCR) process is a method to reduce nitrogen oxides already formed in the flue-gas of a combustion unit. It is operated without a catalyst at a temperature between 850 and 1100 °C. This temperature range strongly depends on the reagent used. It can be ammonia, urea or caustic ammonia. When using ammonia is a reagent, the main reaction is the reduction of NOx to N_2 (reaction 1). However, a side reaction of unwanted oxidation of ammonia may also occur (reaction 2). [Annamalai & Puri, 2007]

1. $\mathbf{4\,NO + 4\,NH_3 + O_2 \rightarrow 4\,N_2 + 6\,H_2O}$
2. $\mathbf{4\,NH_3 + 5\,O_2 \rightarrow 4\,NO + 6\,H_2O}$

At temperatures below that operational window both reactions occur with very low efficiency, but at the higher temperature, the unwanted side reaction dominates with an increase of NO_x emissions as a result. An SNCR installation requires reagent storage unit and SNCR unit itself, which

includes injection of the reagent and reduction of nitrogen oxides to nitrogen and water. There are several injection levels to obtain the required temperature window in the boiler. [1]

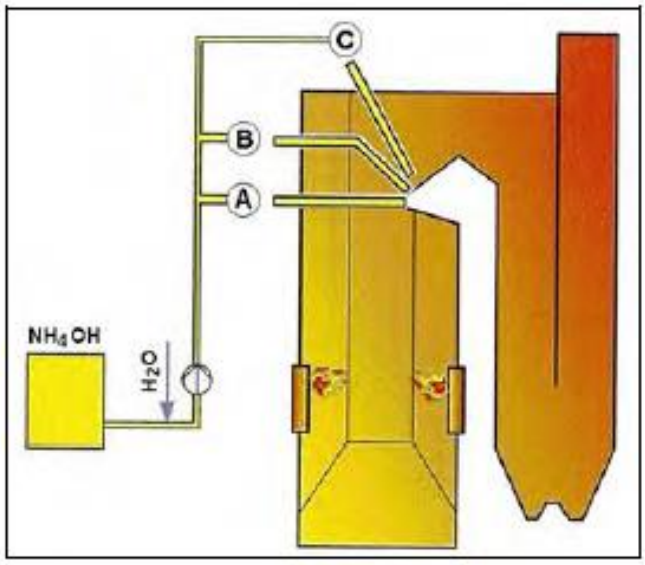

Figure 4 The schematic representation of SNCR process [European Commission, 2006]

High abatement rate and low NH_3 slip may be achieved by the sufficient mixing and appropriate droplets size. The efficiency of the method is estimated at ca. 50%. [Kucowski et al., 1993]

The application of urea in SNCR may cause relatively high formation of N_2O. This, however, may be overcome by injecting it to burnout air instead of primary combustion zone. Urea also leads to more corrosion problems than ammonia, so the materials for such installation and the boiler have to have appropriate properties.

2.2.2 Selective catalytic reduction (SCR)

The selective catalytic reduction is a technique of nitrogen oxides reduction similar to SNCR. It also uses ammonia or urea as reducing agents. Instead of providing very high temperature to match exactly the temperature window of the used reagent, the SCR method uses catalyst to enable reaction to occur with smaller activation energy. Nitrogen oxides reduction takes place on the catalyst surface at temperature between 170-600^{o}C depending on the used catalyst. The reactions occurring in the process are similar to those observed in SNCR. [US DoE, 2004, Busca et al. 1998, Heck & Farrauto, 1995]

$$4\ NO + 4\ NH_3 + O_2 \rightarrow 4\ N_2 + 6\ H_2O$$
$$2\ NO_2 + 4\ NH_3 + O_2 \rightarrow 3\ N_2 + 6\ H_2O$$

The catalysts are used in the form of honeycomb monoliths [Heck & Farrauto, 1995], or plates [Simon, 1995] as illustrated in Figure 5. The used structure enables high flue gas contact surface per volume and low pressure drop. There are four catalyst types used in SCR:

- base metal oxides, which consist of the support material (TiO_2), together with the active components vanadium, tungsten, molybdenum. In most cases, V_2O_5 is used with small amounts of WO_3, added in order to extend the narrow temperature window, small amounts of SiO_2 in order to stabilise the structure and small amounts of MoO_3 in order to make the catalyst more resistant to poisoning from exhaust gas constituents. This type of catalyst has best efficiency in temperature range of 300 – 450 °C.
- zeolites, which are crystalline, highly porous natural or synthetic aluminosilicate three-dimensional structures. Catalysts based on zeolites are used at temperatures between 350 and 600 °C.
- iron oxides, which consist of iron oxide particles with a thin crystalline cover of iron phosphate
- activated carbon, as in eg. in Mitsui method [http://www.mitsui-mining.co.jp/index2.html]. Due to thermal instability of activated carbon at higher temperatures, low operating temperatures of 100 – 220 °C are required. As a result, in power stations, activated carbon can be employed in the 'tail-end' configuration, because only this setting guarantees proper thermal conditions.

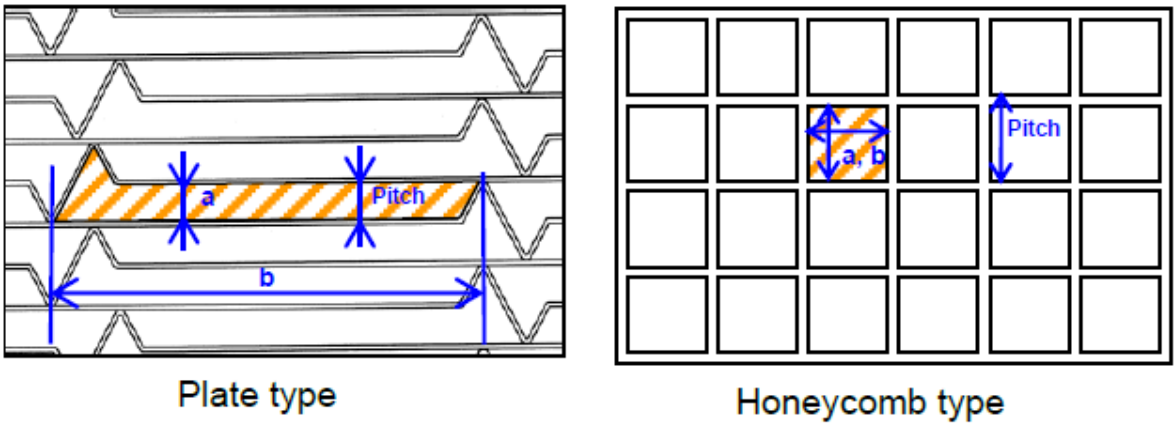

Figure 5 Plate and honeycomb monolith shape comparison [Hitachi, 2012]

SCR catalyst technique can be successfully applied in stationary emission sources, such as large power plants. Depending on situation, there can be three places in exhaust gases stream to install the catalyst bed, as illustrated in Figure 6[Heck & Farrauto, 1995]]:

- High dust – it is most popular one, due to its high operation temperature without the necessity of reheating of flue-gas. The method is characterized by high cost effectiveness. The main drawback of this arrangement is high dust concentration, which can lead to blocking of the monolith channels and deactivation by components of dust (especially heavy metals). Another disadvantage may be catalyst poisoning with sulphur oxides.
- Low-dust – by installing catalyst bed downstream of the electrostatic precipitator, this method avoids most drawbacks of high dust arrangement. However, it requires the installation of high temperature ESP, which can be uneconomic in case of retrofitting old power plants.
- Tail-end – it could be recognized as the advantageous arrangement from the point of view of possible decrease in catalyst lifetime caused by the other two methods. It allows narrower channels in the honeycomb with no danger of blocking. However, the main drawback of this configuration is low temperature of exhaust gas which requires reheating.

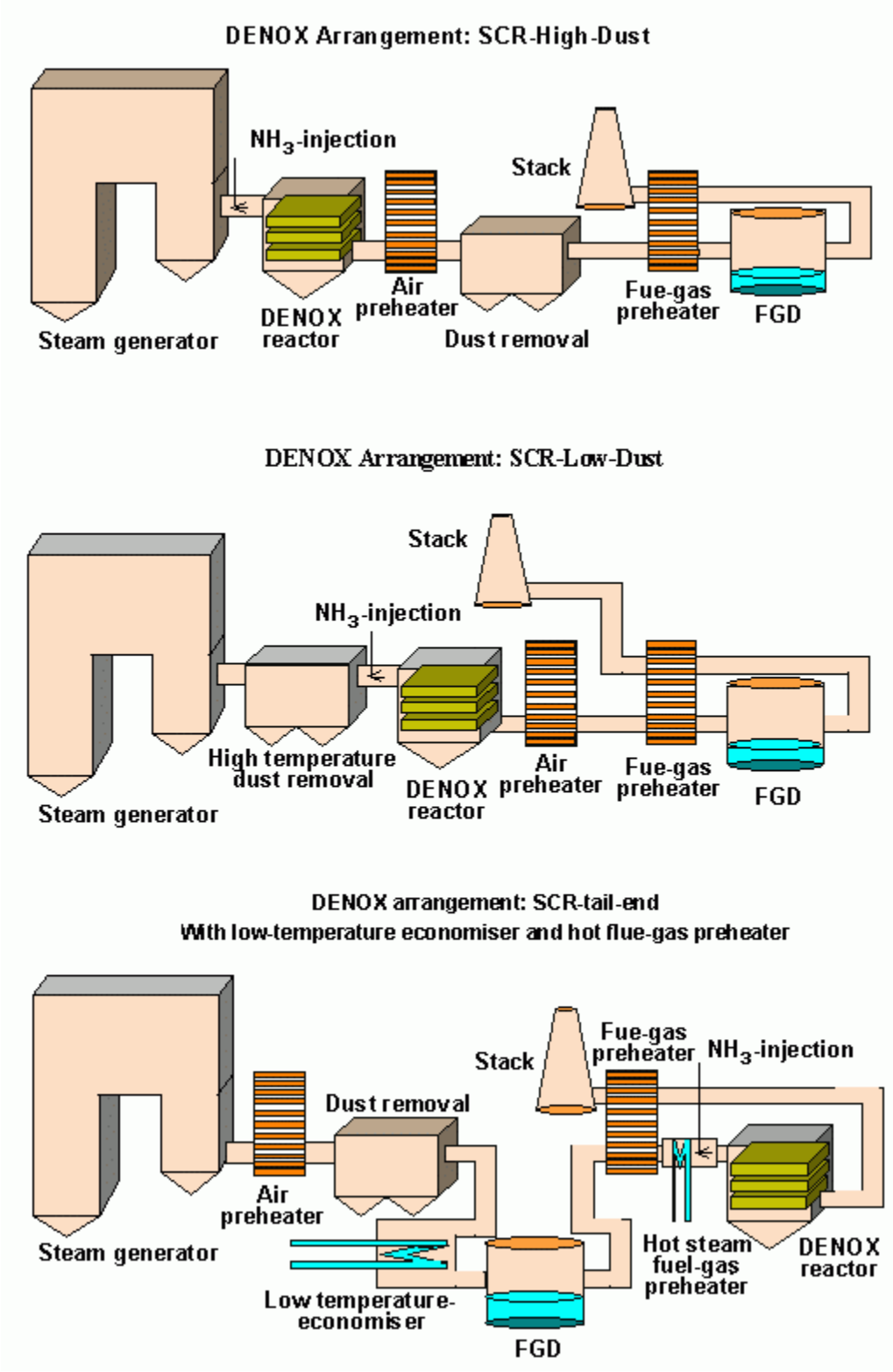

Figure 6 The possible configurations of SCR technologies [European Commision, 2006]

2.3 BAT methods

European Commission Directive explains BAT (Best Available Techniques) as the “means to the most effective and advanced stage of development and methods of operation which indicate the practical suitability of particular techniques providing the basis for emission limit values and other permit conditions designed to prevent and, where that is not practicable, to reduce emissions and the impact on the environment as a whole”. The techniques in question cover both applied methods and the way of designing, maintaining and operation, as well as decommissioning. The main aim of BAT methods is to achieve the highest possible overall environment protection level. [EU directive 2010/75/UE]

For pulverised coal combustion plants, the reduction of NO_x emissions by primary and secondary measures, such as SCR, where the reduction rate of the SCR system ranges between 80 and 95 % is considered as BAT. The use of SCR or SNCR has the disadvantage of a possible emission of unreacted ammonia (‘ammonia slip’). For small solid fuel-fired plants without high load variations and with a stable fuel quality, the SNCR technique is also regarded as BAT in order to reduce NO_x emissions. For pulverised lignite and peat-fired combustion plants, the combination of different primary measures is enough to meet BAT restrictions. This may be realized for example by the application of advanced low NOx burners in combination with other primary measures such as flue-gas recirculation, staged combustion (air-staging), reburning, etc. In fluidised bed combustion boilers burning solid fuel, BAT is the reduction of NO_x emissions achieved by air distribution or by flue-gas recirculation. The newest directive concerning (among others) NO_x emission level is EU Directive 2010/75/EU. The allowed emissions depend on the type of fuel used and the nominal power of the installation in question, as illustrated by Table 1

Table 1 Emission limits for power plants in mg/Nm^3 of NO_x [Directive 2010/75/UE]

Nominal power in fuel[MW]	Coal, lignite and other solid fuels	Biomass and peat	Liquid fuels
50-100	300 450 for lignite	300	450
100-300	200	250	200
>300	200	200	150

3. Catalysts

Catalysts are used in SCR DeNOx method to increase the efficiency. Ammonia and nitrogen oxides molecules are physically or chemically adsorbed on catalyst surface to raise probability of molecules collision. This results in lower activation energy required for the reaction. Original, non-catalytic reaction temperature of NOx reduction with ammonia is between 850^{o}C-1000^{o}C. By using a catalyst reaction, minimal temperature is lowered to a level depending on the catalyst. The second problem solved by using an appropriate catalyst is a desired reaction selectivity. By using proper materials and conditions by-reactions are strongly limited or eliminated.

There are many types of SCR catalysts that have been tested at laboratory scale, but only a few have proven to be efficient and durable enough to be used in pilot plants. For low temperature application catalysts based on activated carbon or carbon fibers were studied [Grzybek et al., 2004, Grzybek et al., 2005]

Commercial DeNOx catalyst available on market, used commonly in coal fired power plants is V_2O_5/WO_3 on TiO_2 support. [Casanova et al., 2012, Willi et al. 1996,Ruggeria et al.,2011,Schwammle et al., 2013]. The necessary element of the catalyst is a so-called monolith (honeycomb), or in certain cases, for flue gasses with especially high ash content, plates are used.

The main difference between both configurations is the ration of amount of surface to volume. The smaller fissure and plates dimensions, the higher the amount of active material contacting flue gases. The same correlation is valid in case of honeycomb shape, by introducing additional walls between plates, square shaped channels are formed instead of fissures. This change creates more durable structure enabling channel walls to be 1 mm thick with 9 mm distance between. In theory smallest diameter should be best, but it leads to practical difficulties, such as pressure drop on catalyst bed and fly ash deposition. Pressure drop has to be compensated by additional air pump, which lowers overall powerplant efficiency. If fly ash concentration in flue gases entering catalyst is very high, small channels may be blocked at entrance, disabling whole following section and significantly lowering catalyst efficiency [Kamata et al., 1998].

Few information on the performance of V_2O_5 – catalysts in industrial installation are available. As an example the work of Simon [Simon, 1995] may be quoted. He describes DeNOx system tested in Duernrohr, first thermal power plant in Austria equipped with SCR reactors. Power station had two units with nominal power of 405 and 352 MW, both fuelled by Polish hard coal and/or natural gas. Catalyst beds, in the form of plates, were placed in high dust configuration and were made of plasma coated steel grid covered by ceramic catalyst material. The installation was described as successful but not without problems. The main issue occurred after 10000 hours of operation in first unit. There was a sudden ammonia slip increase followed by a greater pressure loss in the air heater, downstream of DeNOx installation. The investigation showed that SO_3 from flue gases reacted with

excess ammonia creating ammonium sulphates. This compound can block both the catalyst surface and air preheater.

1.3 Catalyst deactivation

There are three main types of catalyst deactivation: mechanical, thermal and chemical, as illustrated schematically in Figure 7**Error! Not a valid bookmark self-reference.**. They may depend on conditions in catalyst bed, and have consequences of pollution from fuel used for combustion.

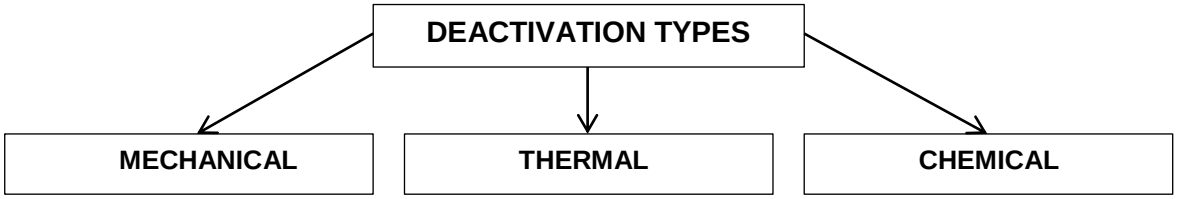

Figure 7 Catalyst deactivation types

1.3.1 Thermal

There are several catalyst bed settings on flue gas route available. Catalyst operation temperature depends on combustion temperature inside boiler and the distance, which exhaust gases have to travel between the boiler and DeNOx reactor. Long exposure can influence both support and active substance. Materials used for support are always in crystal phases that guarantee the highest specific surface for better contact area of reaction. Operating in high temperatures may lead to phase change of support material to less area-developed version. This causes significant drop of catalyst efficiency. Examples of this deactivation mechanism are phase changes of γ-Al_2O_3 to α-Al_2O_3 and anatase to rutile in case of TiO_2.High temperature may also influence active material. As in case of support, transition group metals can create many different structures on catalyst surface. Many studies show that due to thermal deactivation, monomeric vanadium species present on the catalysts may be converted into polymeric species. According to Nova et al. this will result in higher activity but much lower selectivity of SCR catalyst. Polymeric vanadium species have higher influence on SO_2 to SO_3 oxidation and also cause significant increase in the rate of ammonia oxidation. [Nova et al. 2001]

1.3.2 Mechanical

Mineral matter content in coal for powerplants depends on the origin and type of fuel. During combustion most of its mass is converted to ash. Heavier and bigger fractions are transported by gravitation to the bottom of boiler creating bottom ash. Lighter particles are carried by flue gases out of boiler. Every coal powerplant has to be equipped with fly ash removal system to meet the environmental standards. Taking into account that in most powerplants SCR unit is positioned upstream of electrostatic precipitator, ash deposition can be major cause of deactivation, and the resulting efficiency drop rate is the highest. Monolith channels can be successively blocked, increasing the pressure drop on the catalyst bed. Every channel blocked at its entrance excludes significant reaction surface, decreasing overall catalyst efficiency. Thus in some cases, periodical removal of ash with compressed air is applied.

Apart from mechanical deactivation caused by fly ash, chemical effects arising from its composition must be taken into account.

1.3.3 Chemical

Fluegas exiting boiler is carrying oxidised products of combustion as well as light part of ash. Coal used in powerplants contains mainly five elements: C, H, O, S, N, as well as mineral matter. Upon combustion in boiler these elements are converted into CO_2, H_2O, SO_x, N_2 and NO_x. Sulphur compounds may be one of the main reasons other potentially dangerous elements arise from mineral matter.

Sulphur compounds mainly found in flue gases is SO_2, and in low percentage SO_3. Vanadium oxides can increase the undesired conversion of SO_2 to SO_3. Several studies showed that in temperatures lower than 300^{o}C sulphur oxide(VI) can react with ammonia resulting in the formation of $(NH_4)_2SO_4$ and NH_4HSO_4. These compounds may deposit on the catalyst, significantly reducing the surface available for SCR reaction. It was found that 5-10% of tungsten oxide addition may significantly increase sulphur resistance of vanadium catalysts. Other elements increasing resistance towards sulphur were also studied. One of the most promising substitutes could be Sb, which in concentrations of 2% was found to give better results than 10% tungsten, not taking into account other functions of WO_3 addition. [Liua et al., 2010]

Alkali metals such as Na and K are present in fly ash from solid fuels, but much higher concentration were found in ash from biomass. It is because potassium is a part of cell wall structure in plants. Alkali oxides were found to be a very serious danger for vanadium-tungsten catalysts. Studies of Nicosia et al. show that they have ability to influence active material reactivity even if found in small concentrations. Brönsted acid sites, which are crucial to DeNOx reaction, are built as –V-OH.

Potassium and sodium can replace hydrogen from hydroxyl group neutralizing acidic properties and creating –V-OK or –V-ONa species on catalyst surface[Chena et al. 2007]. The second type of alkali deactivation affects vanadium oxidation state. According to the reaction mechanism, in one of the steps $-V^{5+}=O$ species is oxidising $-NH_4^+$ to $-NH_3^+$ reducing itself to $-V^{4+}-OH$ [Kristensen et al. 2011]. In the last step of mechanism, adsorbed oxygen oxidises the reduced group back to the initial state, but lowered acidity of surface caused by alkali poisoning inhibits this reaction, intensifying efficiency drop of catalyst. [Nicosia et al. 2007].

4. Experimental

The main aim was to study the changes in a commercial (propriety) catalyst tested in an industrial installation and to compare the results with the information obtained for laboratory tested (poisoned) catalysts described in literature.

4.1 Samples

EDF Polska R&D department provided four samples of DeNOx catalyst for examination. All samples were exposed to flue gases from the real pulverized coal boiler, which was co-firing coal with biomass, with the biomass mass share ranging from 10 to 15%. Several different types of biomass were added during the studied period (up to 12 months). Flue gases had mean temperature of 420^{o}C. Due to different coals and different types and amounts of biomass, the concentration of pollutants changed over the studied period. The maximum and minimum concentrations of the main pollutants within the studied period are summarized in Table 2. The power plant, where the catalysts were tested and the catalyst itself are confidential information of EDF Polska and will therefore not be mentioned further.

Table 2 The concentrations of NO_x and SO_2 in flue gas during the periods of catalysts exposure

Concentration	NO_x [mg/m^3]	SO_2 [mg/m^3]
Maximum	642	833
Minimum	266	2461
Average over the total exposure time	519	1783

The power plant under consideration is not equipped with SCR installation, so the effect on the catalyst was studied after exposure to real flue gases. During trials the catalyst samples were installed directly inside the boiler, just above the water heater of the second pass of boiler (Figure 8, position A). Tested samples were removed after approx. equal periods of time, given below.

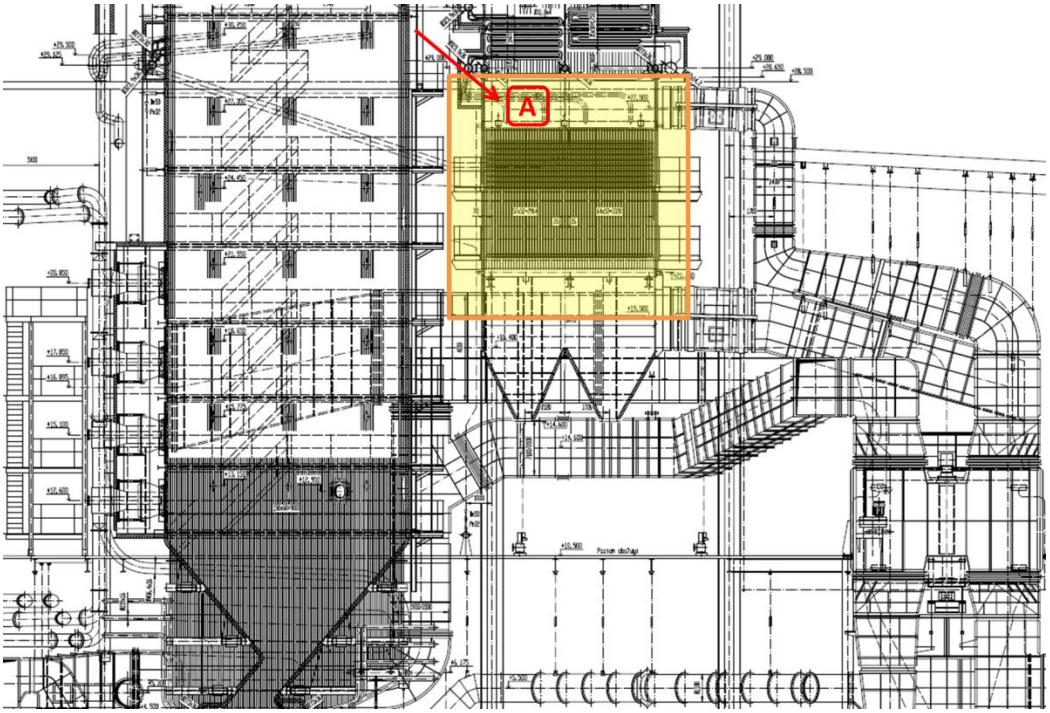

Figure 8 Scheme of flue gases route with marked place (A) of catalyst samples

The samples were delivered by EDF in the form of honeycomb monoliths. Most of them contained fly ash in the channels, as the catalysts were installed in the high dust position. Some of channels were blocked entirely by slightly sintered ash, as shown in Figure 9.

The samples obtained had different times of exposure:

- Fresh sample – a reference sample, before exposure (0M)
- Sample 3M – after 2270 hours operation
- Sample 6M – after 4527 hours operation
- Sample 12M – after 9405 hours operation

Each monolith had a cross section of 9 per 18 square channels. Despite protection granted by metal casing, outside layer of channels in each sample was partly destroyed, because of transportation conditions and difficulties connected to extracting the used catalyst from their bed inside boiler.

Figure 9 The catalyst monolith in steel casing after exposure to flue gas for 9405 hours

For experimental techniques requirements a part of the samples material was grinded manually with use of the agate mortar. Before this procedure, non-bonded fly ash was collected from samples 3M, 6M and 12M and labelled 3M ash, 6M ash and 12M ash, respectively, as given in Table 3. The ash samples were also tested in order to compare them with the appropriate catalysts. To provide representative samples for examination, the monoliths were cut, as illustrated in Figure 10, taking the material from outer and inner parts of the monoliths in suitable proportions. Such prepared samples were kept in hermetic containers for further investigation.

Table 3 Sample designation and description

Sample name	Sample description
0M	Reference sample
3M	Catalyst sample after three months of operation
6M	Catalyst sample after six months of operation
12M	Catalyst sample after twelve months of operation
3M ash	Ash collected from 3M
6M ash	Ash collected from 6M
12M ash	Ash collected from 12M

Figure 10 Catalyst samples preparation

4.2 Characterization methods

Catalysts, both fresh and exposed to flue gases in the power station, as well as the samples of collected ash were characterized. All samples were investigated by the chosen methods, if not otherwise. The following methods were used:

- Atomic absorption spectrometry (AAS) – to determine the content of selected elements for the collected ash samples
- Scanning electron microscopy (SEM)/ Electron Dispersive Spectroscopy (EDS) – to study the morphology of fresh and exposed catalysts, as well as a selected ash sample
- X-ray diffraction (XRD) – to determine the phase composition
- UV-Vis – to find out the changes in the exposed catalysts in comparison to the fresh one
- Horizontal Attenuated Total Reflectance Fourier Transform (HATR-FTIR) – to study surface groups
- Butene isomerisation – to determine the changes in acidity of catalysts after exposure.

4.2.1 AAS

Atomic Absorption Spectrometry is a measuring technique used to determine the bulk quantity of a given element in a sample. This technique is based on the phenomenon of absorption specific radiation by elements in atomic state. The equipment used includes

- an atomiser converting the sample into atomic state. It can be realized by flame or electrothermal atomizer
- radiation emitter to form radiation beam with proper wavelength corresponding to the tested element
- a detector, which measures radiation intensity obtained from the sample. By comparison of radiation intensity, the element concentration can be determined using Lambert-Beer law [Royal Society of Chemistry, 2000][Garcia & Baez, 2012]:

$A=k*c*l$

where:

A – absorbance[-]

k – absorbance coefficient [dm^3 /cm*g]

c – concentration of measured element in absorbing layer [g/dm^3]

l – thickness of the absorbing layer [cm]

Absorbance may be recalculated to concentration, by the comparison with the appropriate standard. AAS was performed to confirm presence of poisoning elements in catalyst and ash. The following samples were measured: 0M, 3M, 6M, 12M, 3M ash, 6M ash and 12M ash. The content of Si, Al, Ca, Fe, Mg, K and Na was analysed. The samples were digested in concentrated HNO_3 and HF acids in Berghof microwave digestion system - Speedwave Four. Atomic absorption spectrophotometry with the use of flame atomization was carried out by Hitachi Spectrophotometer Z-2000 with Zeeman effect background correction and HCL (hollow cathode lamp) as the source of radiation. For the determination of Fe, Mg, K and Na, the standard burner, fed with acetylene and air, was used for atomization. Because of high temperature of Si, Al and Ca atomization, high temperature burner fed with nitrous oxide, acetylene and air was used.

4.2.2 SEM/EDS

A scanning electron microscope (SEM) is an instrument that produces images of a sample by scanning it with a focused beam of electrons. Electron beam interacts with atoms on the surface, forcing them to emit signals carrying information about sample's composition and surface topography. The detected signal with cooperation with beam position results in SEM image. Specific X-ray radiation may be measured by electron dispersive spectroscopy (EDS) detector to determine sample composition at a given point. The resolution available for this method may be even lower than 1 nm. Depending on the equipment type, the measurement conditions are high vacuum, low vacuum, wet conditions in case of environmental SEM, and a wide range of temperatures from cryogenic to hot measurements. [Reed, 2005][Hafner, 2007]

The morphology of the fresh and exposed catalysts was analyzed with the Joel JSM7001F FEG-SEM with an Oxford energy dispersive X-ray high vacuum detector (E = 20 kV) for elemental microanalysis. The collected ash sample was also examined. The powder samples studied over double face carbon adhesive (analytical grade) were covered with a thin film of graphite.

4.2.3 XRD

X-ray diffraction is a technique based on the Bragg's Law and is used among others to identify compounds in crystal form. A sample in the form of a single crystal or compressed powder disc is mounted in the goniometer, which allows high precision aligning of the sample with the radiation beam The angle between the beam and the sample surface is controlled by goniometer rotation. The Braggs equation allows to determine the distance between atomic layers and, as a consequence, crystallographic structure of the studied material:

$$n\lambda=2d\sin\Theta$$

where:

n – diffraction order, small integer

λ – X-ray wavelength

d – distance between atomic layers

Θ – angle between radiation beam and the normal to sample surface

As λ is fixed in the experiment, and Θ is measured, the value of d may be determined. Each crystalline compound is characterized by a unique diffraction pattern, thus allowing its identification. The measurement is performed by changing the angle of incident X-ray beam. As a result, the

diffractogram is generated, giving diffracted radiation intensity for a set angle. Apart from identification of a certain compound, XRD allows to determine the crystallographic structure of unknown compounds, cell parameters, phase analysis as well as the size of crystallites. [Zachariasen, 1967][Warren, 1990]

XRD measurement was performed for all studied catalysts and ash from all exposed catalysts with PANanalytical Empyrean diffractometer using CuK alfa ration (λ = 154.05 pm) at room temperature.

4.2.4 UV-vis

Ultraviolet-visible spectroscopy is one of the oldest analytical methods in chemistry. It is based on the phenomenon of light absorption. It can be used both to identify compounds and to measure their quantity, it may be used for both solutions and solids. A beam of radiation with the wavelength from 200-800 nm is either transmitted through solution with suspended sample particles or reflected from a surface of solid sample. In both cases, the next step is to split the beam into rays with different wavelength. The intensity of radiation of each wavelength is measured and compared to a reference sample with zero absorbance. The result of UV-Vis spectrophotometry is a spectrum representing absorbance of radiation for given wavelength versus the measured range of radiation. The absorbance peaks can be identified using a database. [Padera, 2013]

The diffuse reflectance UV–VIS spectra, of fresh, 3M, 6M and 12M catalysts were obtained using a Cary 5000 Varian equipment with a DRA 2500 diffuse reflectance accessory (integration sphere) to identify changes of active phase caused by the exposure to the flue gas.

4.2.5 HATR-FTIR

Infrared spectroscopy is a group of methods using infrared radiation to obtain oscillation spectrum of compounds. Infrared spectroscopy can be used to analyse both molecular structure and its interference with environment. When transmitted through the measured sample, a part of radiation is selectively absorbed, increasing the amplitude of oscillation. Molecule symmetry determines which oscillations will give absorption peaks in the obtained spectrum. Oscillation energy is quantified and thus only specific energy radiation can be absorbed, characteristic of oscillating functional groups. Those characteristic wavenumbers are summarized in tables to enable identification. The selection rule for the IR is the change in dipole momentum.

Fourier transform allows the registration of the whole IR spectrum at once, instead of discrete wavelength changing during the measurement. Spectrum transmitted through a sample is combined with the initial radiation, creating an interferogram, which is recalculated to a spectrum using Fourier transform.

Horizontal attenuated total reflectance (HATR) is a relatively recent variation of FTIR instruments. It is very useful in obtaining the spectra of solids, without the use of support materials, such as e.g. KBr. This method is based on the internal reflection of IR radiation by a measured material. The sample is pressed against an appropriate crystal and the radiation from the source penetrates a very small distance into the sample. During the penetration of the IR radiation, energy is absorbed by the sample at wavelengths characteristic for its molecular structure, before being reflected from the crystal to the detector. HATR spectra are therefore similar, but not identical, to transmission spectra. The same wavenumbers are absorbed, but the intensities may vary.[Thermo Nicolet Corporation, 2001]

Infrared spectra of the all catalysts and ashes were collected with a resolution of 16 cm^{-1}, using a FT-MIR equipment from BOMEN (FTLA2000-100, ABB) with a DTGS detector. A horizontal total attenuated reflection accessory (HATR), from PIKE Technologies, with a ZnSe crystal was applied. Sixty-four scans were accumulated for each spectrum to obtain an acceptable signal-to-noise ratio.

4.2.6 Butene isomerisation

Butene isomerisation is one of the methods allowing to compare the amount of acidic sites on a given material. It is based on the fact, that the mentioned reaction is catalysed by acid sites. For a given concentration of n-butene, the amount of 2-butene is measured. The amount of 2-butene obtained in the given below reaction, allows to determine acidity of the sample. [Seo et al. 1995][Van Donk et al. 2001]

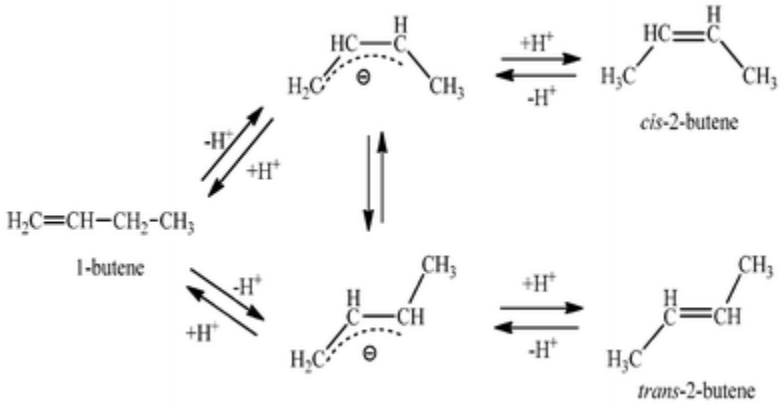

Figure 11 1-butene isomerisation mechanism [Chen et al. 2012]

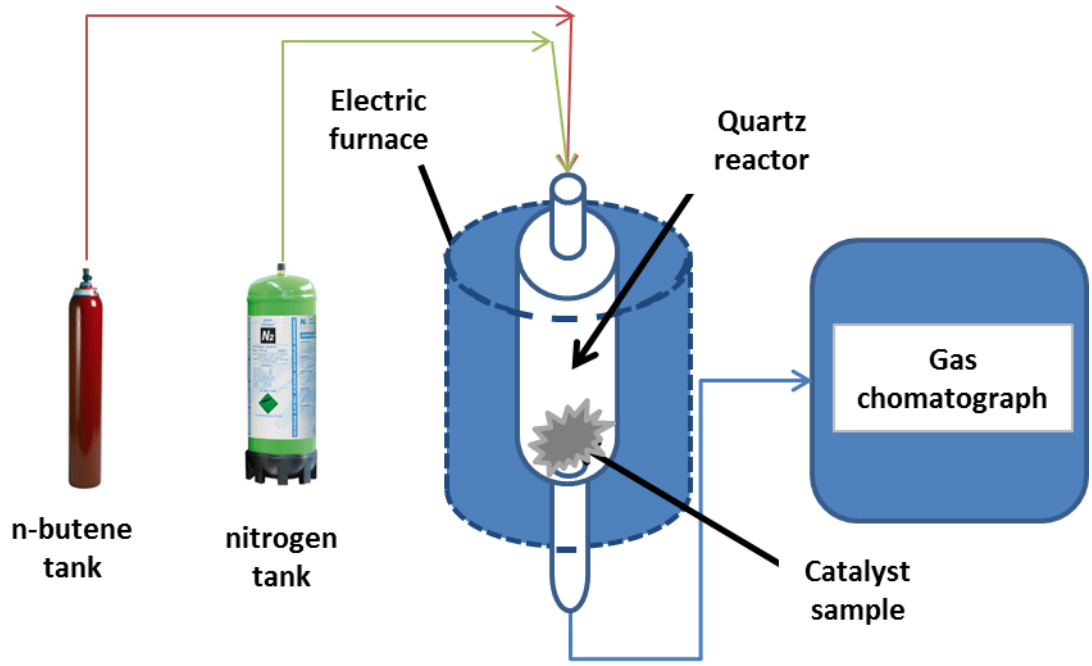

Figure 12 Schematic representation of butene isomerisation aparatus

Therefore for the known initial n-butene concentration, the amount of resulting 2-butene can be measured. The experiment is carried out in the equipment schematically shown in Figure 12 as follows: a weighted catalyst sample was placed in vertical quartz reactor with the thermocouple in the catalyst zone, immobilized by glass wool. Butene was fed from upper entrance and product gases were collected from the bottom. The reactor is heated by an electric furnace. The reaction products obtained at desired temperatures are analysed by gas chromatography.

For each catalyst sample measurements were taken twice at each of four temperatures. The acidity of the studied catalysts was estimated under the following conditions: mass of the sample 0.5g; the composition of reaction mixture fed to reactor was 25cm^3/min of N_2 and 19cm^3/min of 1-butene; the products for chromatographic analysis were collected twice for each selected temperature of reaction: 187^{o}C, 200^{o}C, 225^{o}C and 250^{o}C. The results were presented as efficiency curve as a function of temperature, in order to observe the changes of acidity at different times of operation. The conversion was calculated as:

$$\eta=[\text{2-butene (cis+tras)}]/[\text{initial 1-butene}]$$

where:

η – conversion

[2-butene] – concentration of 2-butene after reaction

[initial 1-butene] – concentration of 1-butene before reaction

5. Results and discussion

5.1 Conversion of NO_x on fresh and poisoned catalysts

The activity of catalysts: 0M, 3M, 6M and 12M was measured during test campaigns in an external laboratory, ordered by EDF Polska. The gas composition during tests was as presented in Table 4; flow [m3/h]: 63 (fresh catalyst) and 66 (catalysts after exposure to flue gas at industrial installation); temperature measured upstream and downstream of catalyst bed in [^{o}C]: 374/343 (0M.); 361/335 (3M); 345/319 (9M); 364/335 (12 M). The results were presented in Figure 13 as a relative loss of activity, calculated as:

$$\Delta x = \frac{(x_o - x_t)}{x_o} * 100\ \%$$

Where: Δx – relative loss of activity

x- conversion

indexes: 0 – fresh catalysts, t– catalyst after time t of exposure: 2270, 4527 or 9405 h

The most significant loss of activity was observed during the first 6 months of operation. Three points representing this period, including the fresh catalyst with relative loss of activity equal to zero, form a straight line with R^2=0.9972. The calculated average relative loss of activity for 6 months was ca 4.2 %/1000 h. It is clear that for the period from 6 to 12 months the rate of deactivation was much lower. Similar results were obtained by Wieck et al. [Wieck et al. 2000] while testing a SCR catalyst deactivated by the operation in boiler fuelled by a coal and straw mixture.

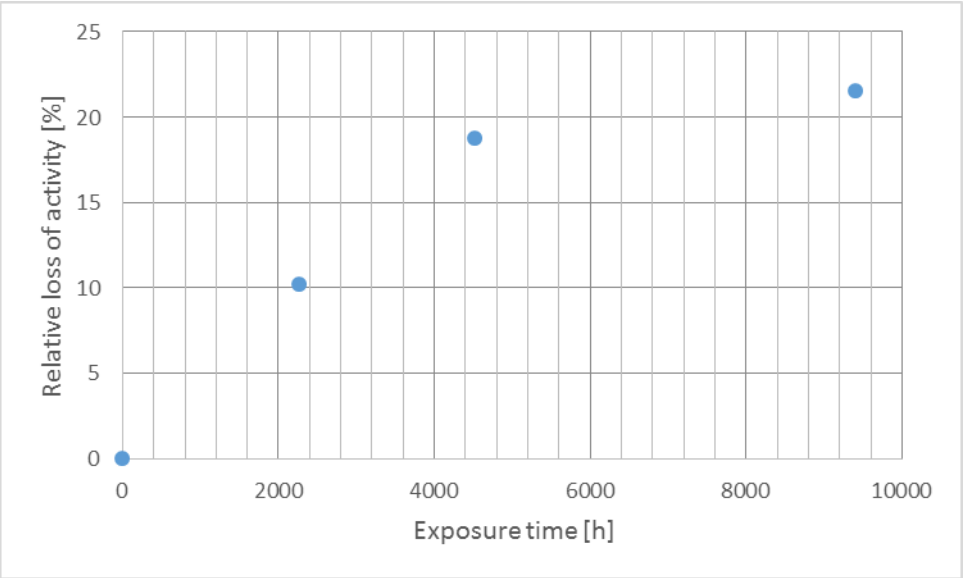

Figure 13 Relative loss of activity of the studied catalysts (the data obtained from EdF Polska)

Table 4 Flue gas composition in conversion measurement (the data obtained from EdF Polska)

Gas composition	CO2, vol%_wet	CO, ppm_wet	SO2, ppm_wet	NOx, ppm_wet	Fly ash g/Nm3
minimum	7.99	463	101	167	20
maximum	9.83	1221	281	215	30

5.2 AAS

Atomic absorption spectroscopy was performed to determine the concentration of the selected elements, identified in the literature [Nicosia et al. 2007] as possible poisons arising from biomass combustion: Ca, Fe, Mg, K and Na. The same elements, together with Si and Al, were also determined for the samples of ash collected from the exposed catalysts. Table 5 and Table 6 present the results of AAS analysis for the studied catalysts and the ash samples collected from the catalysts exposed to flue gas in the power plant.

Table 5 Catalyst composition results from AAS

	0M %	3M %	6M %	12M %
Ca	0.84	1.03	1.12	0.80
Fe	0.04	0.04	0.05	0.53
Mg	0.09	0.09	0.11	0.44
K	0.02	0.10	0.18	0.63
Na	0.01	0.06	0.11	0.34

Table 6 Ash composition results from AAS

	3M ash [%]	6M ash [%]	12M ash [%]
Si	41.73	41.11	49.32
Al	20.35	16.99	20.44
Ca	7.47	4.37	3.16
Fe	6.37	6.87	6.09
Mg	2.72	2.63	2.20
K	2.42	2.43	2.71
Na	0.52	0.65	0.67

From Table 5 Catalyst composition results from AAS it may be seen that:

- Fresh catalyst had only traces of iron, magnesium, potassium and sodium, and a relatively high content of calcium. The exposed catalyst samples were enriched in K and Na, two elements considered the as the greatest poisons of vanadium-based catalysts. Similar results were obtained by Larsson et. al. [Larsson et al. 2007] for a commercial catalyst operating in a full scale biomass combustion plant. Fresh catalysts contained 0.03% of K while 0.5% were registered after 6500 hours (9 months) of exposure.
- Especially high increase in iron concentration between 6M and 12M of exposure was registered. This may possibly come from higher content of F_2O_3 in biomass in this period.
- The amount of calcium changed only slightly during the whole exposure time. Taking into account the composition of the fresh catalyst, it may be assumed, that this element was inherent to the catalyst and only to a small extent may have arised from the ash samples, although wood pellets contain Ca.

From Table 6 it may be seen that ash composition varied between: Si 41.11-49.32%, Al 16.99-20.44%, Ca 3.16-7.47%, Fe 6.09-6.87%, Mg 2.20-2.72%, K 2.42-2.71% and Na 0.52-0.67%. Similar results were obtained by Koukouza et. al.[Koukouza et. al. 2007] who examined fly ash from combustion of Polish coal or wood chips and co-combustion of Polish coal with wood chips in a pilot scale fluidised bed boiler. This study showed that the fly ash from the traditional fuel contained up to 1.67% of potassium while the pure biomass might contain over 12% of K. Taking this number as an

assumption, together with 13% of biomass share in the fuel in the considered EDF power plant, ash with up to ca. 3% mass of potassium, may be expected. It must be pointed out however, that the discussed power plant used a variety of biomass and different types of biomass have different composition.

A comparison between two types of biomass: straw and wood chips is given in Table 7. As discussed in literature [Chen et al. 2006] elevated content of potassium in ash most probably arises from biomass addition to standard coal fuel. Chen et al. studied the content of alkalis in catalyst exposed to aqueous solutions of Na, K, Mg and Ca hydroxides and concluded that K transferred to fly ash, together with K present in co-combusted coal creates a serious threat of poisoning. This study showed additionally that the poisoning potential of alkalis forms sequence: K>Na > Ca >Mg.

Table 7 Composition of biomass from straw and wood chips [Zheng et al. 2005]

Fuel data for Danish cereal straw and wood chips				
composition (wt.%) on dry basis	Straw		Wood chips	
	Typical	Variation	Typical	Variation
Ash	4.5	2–7	1	0.3–6
Volatiles	78	75–81	81	70–85
Hydrogen, H	5.9	5.4–6.4	5.8	5.2–6.1
Carbon, C	47.5	47–48	50	49–52
Nitrogen, N	0.7	0.3–1.5	0.3	0.1–0.7
Sulphur, S	0.15	0.1–0.2	0.05	<0.1
Chlorine, Cl	0.4	0.1–1.1	0.02	<0.1
Silicon, Si	0.8	0.1–1.5	0.1	<1.1
Aluminium, Al	0.005	<0.03	0.015	<0.1
Iron, Fe	0.01	<0.03	0.015	<0.1
Calcium, Ca	0.4	0.2–0.5	0.2	0.1–0.9
Magnesium, Mg	0.07	0.004–0.13	0.04	<0.1
Sodium, Na	0.05	<0.3	0.015	<0.1
Potassium, K	1	0.2–1.9	0.1	0.05–0.4
Phosporus, P	0.08	0.03–0.2	0.02	<0.1

On the other hand, these results indicate that Ca could not, or only to a minor extent, have added to the poisoning of catalysts, despite its high content in fly ash (3.16-7.47%).

5.3 SEM/EDS

Scanning electron microscopy was performed to determine the morphology of the studied samples and to compare the changes caused by exposure to industrial flue gases. Figure 14 and Figure 15 show SEM images of the catalyst samples: Fresh, 3M, 6M, 12M, as well of 6M ash species.

In Figure 14**Error! Reference source not found.** the small objects of fairly regular shapes, as ell as needle-shaped objects much different from rest of particles can be observed for all catalysts samples. It may be observed in Figure 15 that they are coming from the catalyst nodules. They may thus be parts of the monolith, which were originally embedded inside the honeycomb structure. As shown by EDS measurements, they are composed of silicon, aluminum, calcium and magnesium. Titanium registered by EDS belongs probably to support particles.

SEM image of ash presents spherical particles, including empty broken sphere. These may be cenospheres which are often observed as a component of fly ash from coal combustion. Their composition includes typical mineral matter elements, such as silicon, aluminium, magnesium and calcium. Additionally to cenospheres, other ash particles with less regular shapes may be observed.

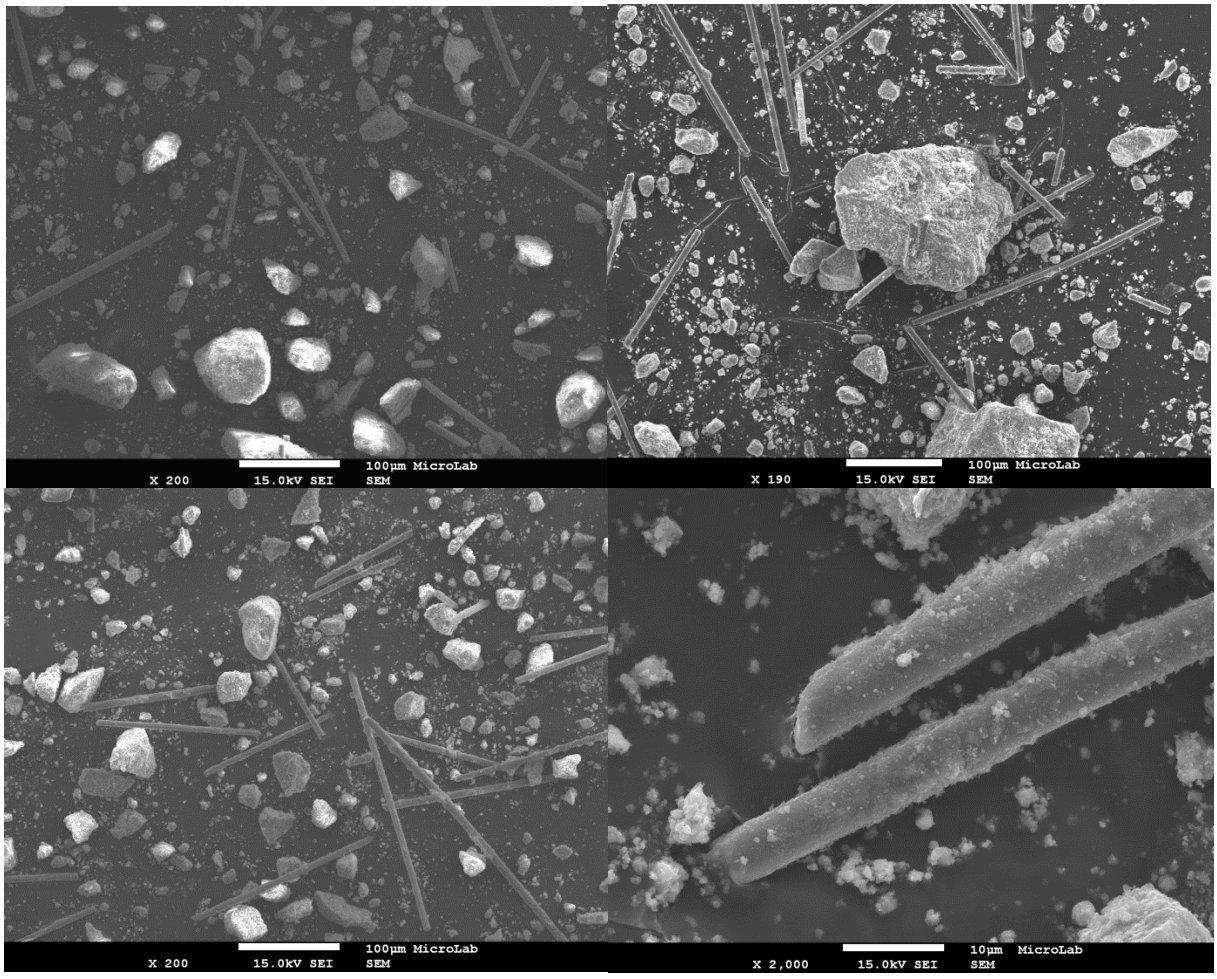

Figure 14 SEM images of needle species on 0M (upper left), 3M (upper right), 6M (lower left) and 12M catalyst (lower right)

In order to analyse the elemental composition and compare the results with those from AAS, EDS analysis was carried out. Additionally, EDS was used to obtain information about the content of

another very important poisoning element that may be present on the surface, that is sulphur. SEM images of fresh and exposed catalysts, as well as of fly ash removed from 6M ash sample are presented in Figures 16-25 and Tables 8-17. For each sample the EDS analysis was carried out at 2 (or in one case 3) selected places, as indicated by SEM images. To compare the elemental composition, concentrations of most important elements for each sample and selected place were summarized in Table 18.

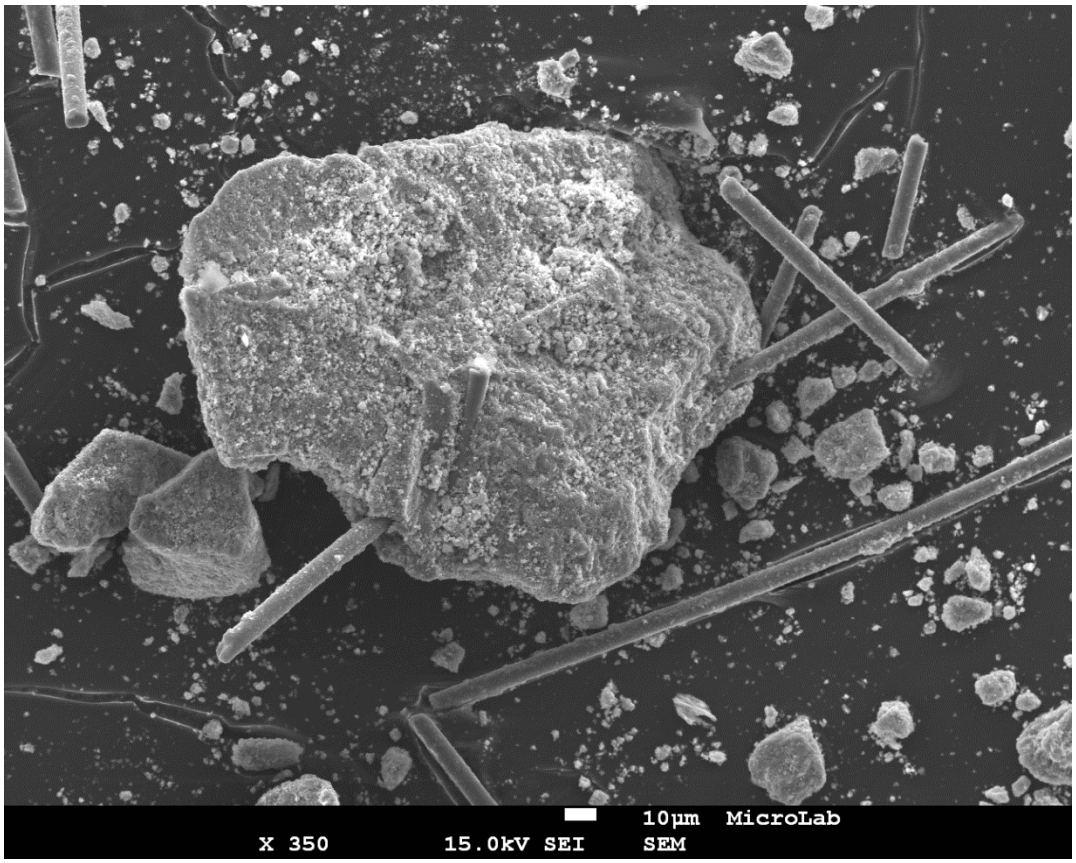

Figure 15 SEM image of needle species connected with catalyst nod

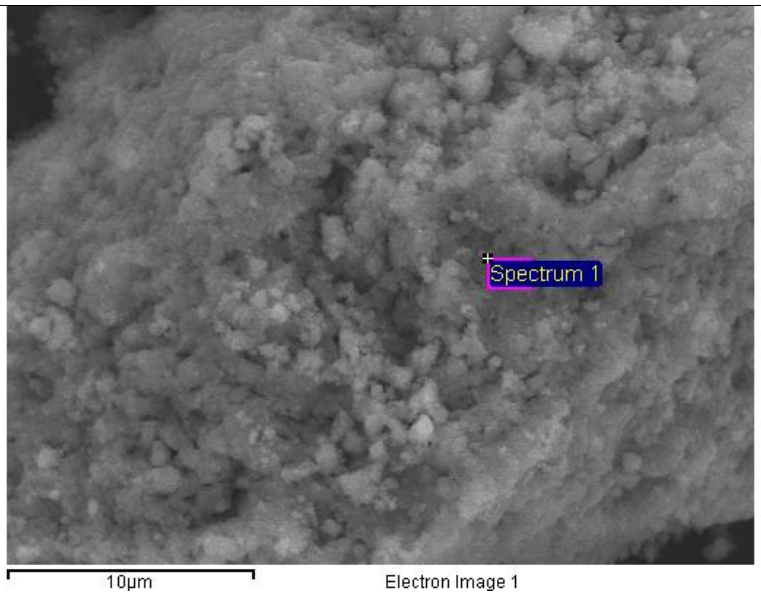

Figure 16 SEM image of fresh catalyst I

Table 8 Results from EDS of fresh catalyst

	Weight%	Atomic %
C	1.42	3.24
O	36.88	63.1
S	0.42	0.36
Ti	56.01	32.01
V	1.29	0.69
W	3.97	0.59

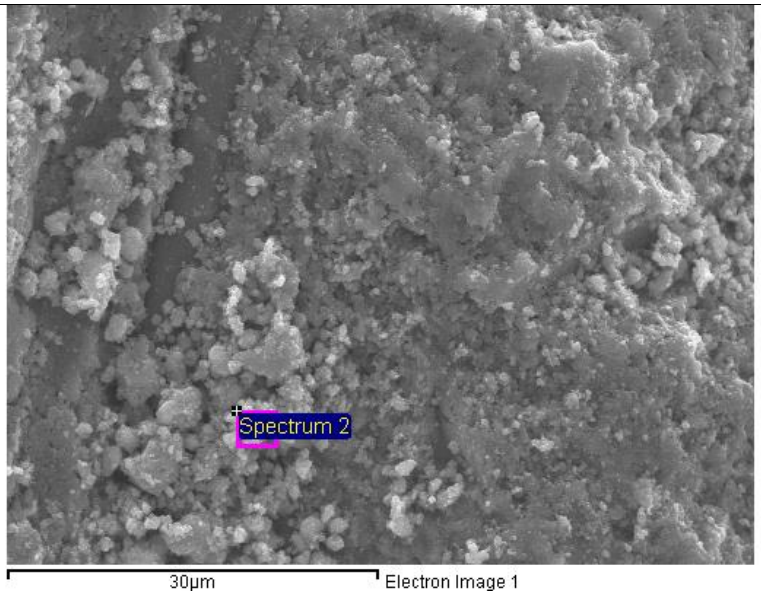

Figure 17 SEM image of 3M catalyst I

Table 9 Results from EDS of 3M catalyst I

	Weight%	Atomic %
C	2.56	5.67
O	36.82	61.29
Al	0.4	0.39
S	0.99	0.83
Ti	56.2	31.25
V	0.38	0.2
W	2.66	0.39

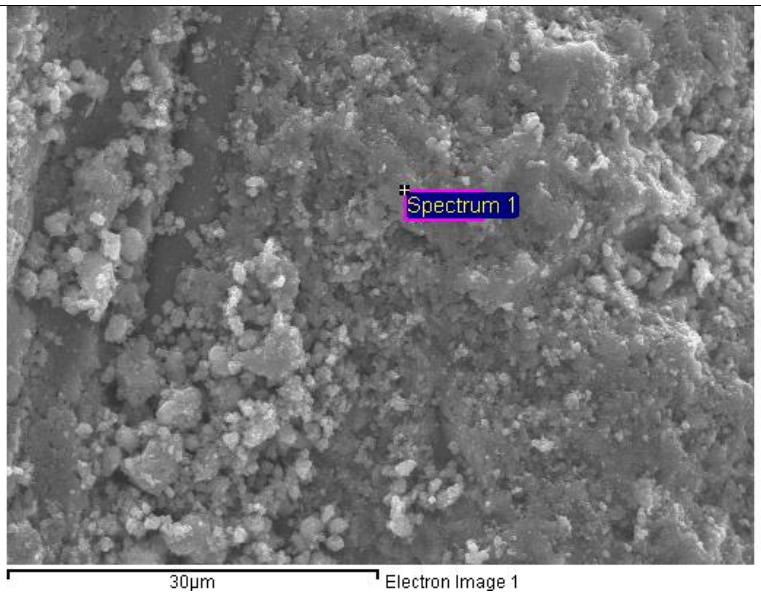

Figure 18 SEM image of 3M catalyst II

Table 10 Results from EDS of 3M catalyst II

	Weight%	Atomic %
C	2.56	5.67
O	36.82	61.29
Al	0.4	0.39
S	0.99	0.83
Ti	56.2	31.25
V	0.38	0.2
W	2.66	0.39

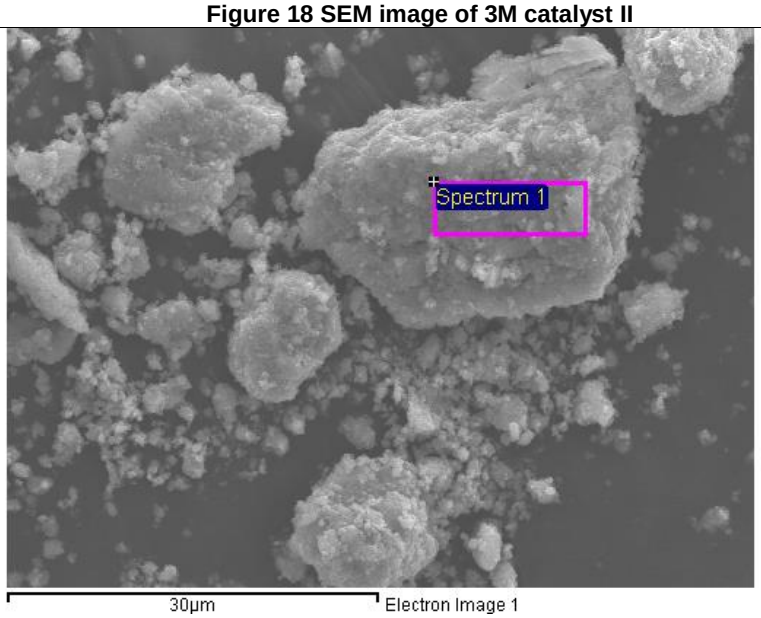

Figure 19 SEM image of 6M catalyst I

Table 11 Results from EDS of 6M catalyst I

	Weight%	Atomic %
C	0.99	2.38
O	33.3	60.09
S	0.32	0.29
Ti	59.96	36.13
V	0.63	0.36
W	4.8	0.75

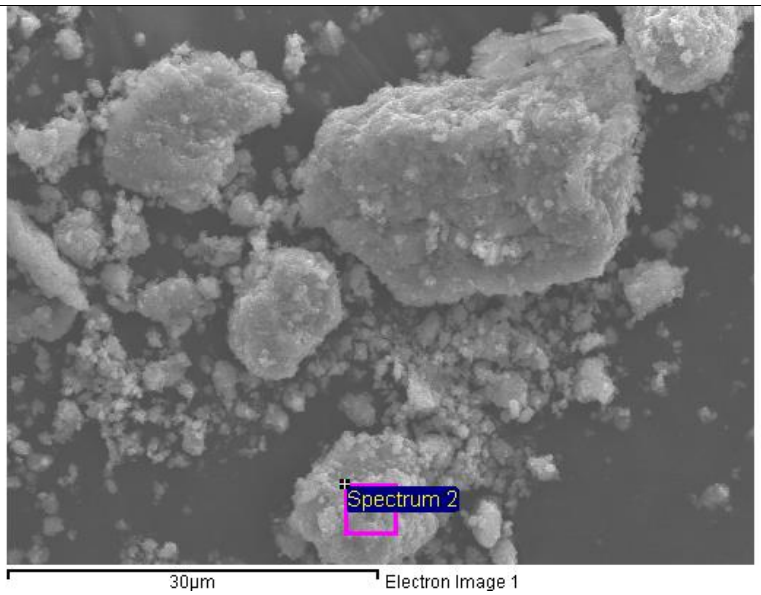

Figure 20 SEM image of 6M catalyst II

Table 12 Results from EDS of 6M catalyst II

	Weight%	Atomic %
O	44.91	72.36
S	0.55	0.44
Ca	0.53	0.34
Ti	47.06	25.33
V	1.5	0.76
W	5.45	0.76

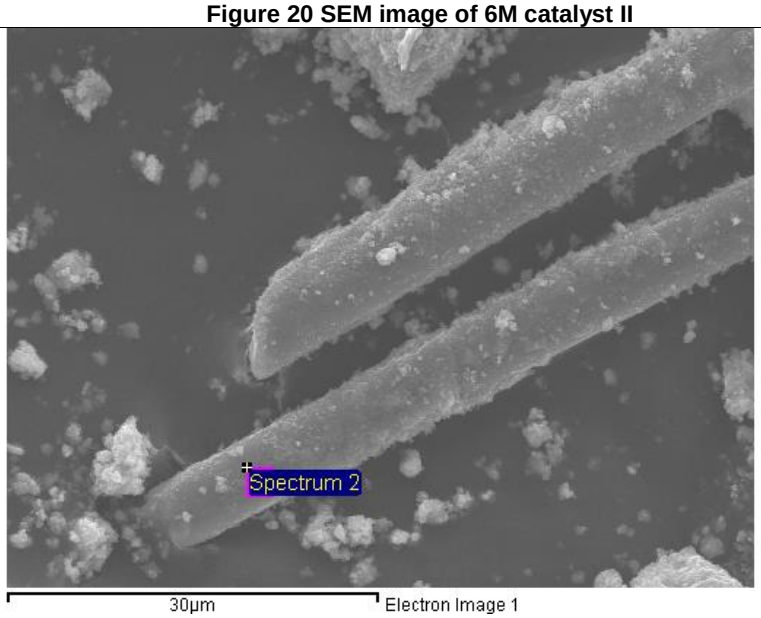

Figure 21 SEM image of 6M catalyst III

Table 13 Results from EDS of 6M catalyst III

	Weight%	Atomic %
O	47.1	63.46
Mg	2.14	1.89
Al	6.79	5.42
Si	25.73	19.75
Ca	14.38	7.73
Ti	3.87	1.74

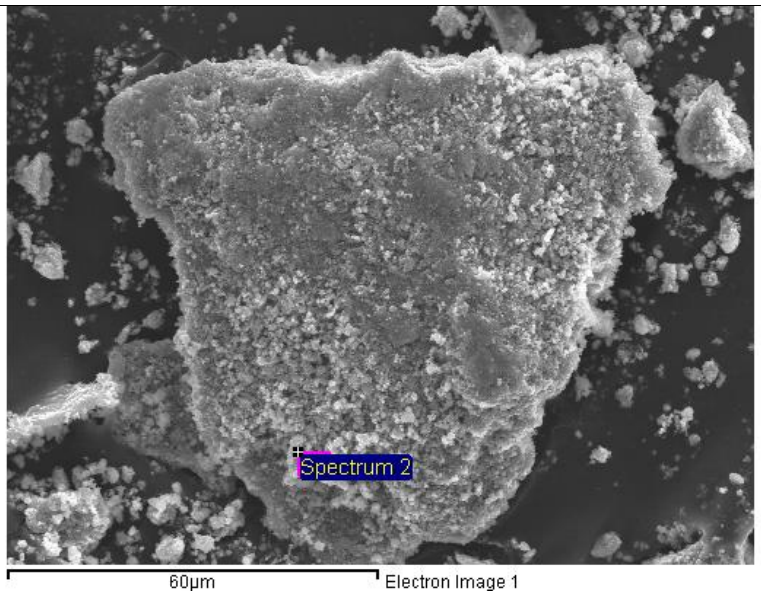

Figure 22 SEM image of 12M catalyst I

Table 14 Results from EDS of 12M catalyst I

	Weight%	Atomic %
C	3.67	7.63
O	41.05	64.05
S	1.25	0.98
Ti	50.9	26.53
V	1.09	0.54
W	2.03	0.28

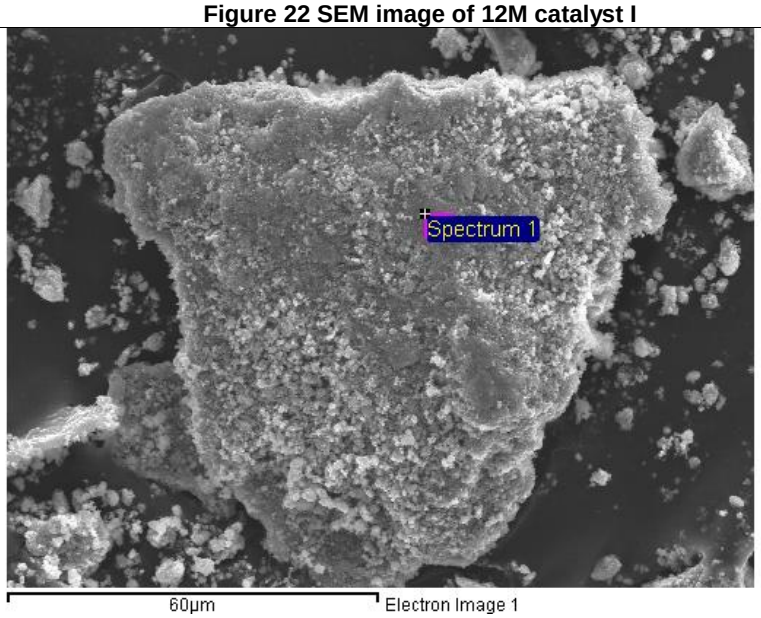

Figure 23 SEM image of 12M catalyst II

Table 15 Results from EDS of 12M catalyst II

	Weight%	Atomic %
C	12.7	25.55
O	30.24	45.68
S	1.54	1.16
K	0.56	0.35
Ti	52.73	26.6
V	1.07	0.51
W	1.17	0.15

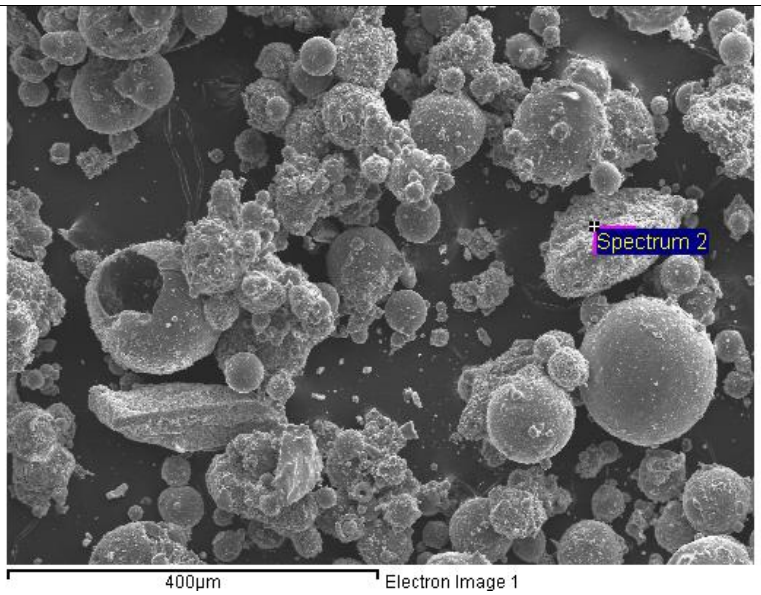

Figure 24 SEM image of 6M ash sample I

Table 16 Results from EDS of ash sample I

	Weight%	Atomic %
C	31.46	43.23
O	39.69	40.95
Mg	0.34	0.23
Al	7.36	4.5
Si	12.71	7.47
S	3.02	1.55
K	2.85	1.2
Ca	0.5	0.21
Ti	0.79	0.27
Fe	1.29	0.38

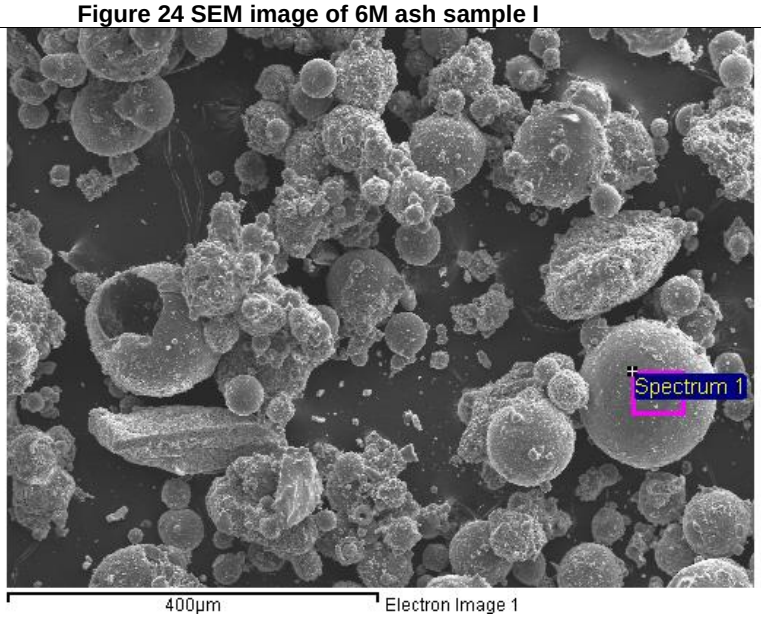

Figure 25 SEM image of 6M ash sample II

Table 17 Results from EDS of ash sample II

	Weight%	Atomic %
C	21.6	32.57
O	37.99	43.01
Na	0.43	0.34
Mg	0.75	0.56
Al	9.43	6.33
Si	20.64	13.31
S	1.74	0.98
K	3.21	1.49
Ti	0.89	0.34
Fe	3.31	1.07

For every sample, except 6M ash, a typical place with the composition including Ti, V, W, O and thus identifying it as a part of catalyst was found. Additionally most analysed places contain carbon. However, it is not possible to determine if it is unburned fuel because of the procedure of sample preparation for SEM. Apart from the pollutants already identified by AAS i.e. K and Na (cp. Table 5 and Table 6), considerable amounts of S were identified by EDS. Sulphur is present even in the fresh catalyst.

Table 18 The comparison of the content of K, Na and S from EDS measurements (I and II = spectrum at place 1 and place 2 in SEM images)

	0M	3M		6M		12M		Ash	
	I	I	II	I	II	I	II	I	II
	Weight %	Weight %	Weight %	Weight %	Weight %	Weight %	Weight %	Weight %	Weight %
S	0.42	0.57	0.99	0.32	0.55	1.54	1.25	1.74	3.02
K	0	0	0	0	0	0.56	0	3.21	2.85
Na	0	0	0	0	0	0	0	0.43	0
	Atomic%	Atomic%	Atomic%	Atomic%	Atomic%	Atomic%	Atomic%	Atomic%	Atomic%
S	0.36	0.83	0.43	0.29	0.44	1.16	0.98	0.98	1.55
K	0	0	0	0	0	0.35	0	1.49	1.2
Na	0	0	0	0	0	0	0	0.34	0

5.4 XRD

X-ray diffraction of four catalyst samples (0M, 3M, 6M and 12M) and three ash samples (3M ash, 6M ash and 12M ash) was carried out to determine the phase composition. The obtained XRD patterns shown in Figures 26, 27, 28 and 29 for the studied catalysts and ash samples scraped from the appropriate exposed catalysts were compared to database model compounds.

Figure 26 shows the same reflections for all catalyst samples, which were identified as TiO_2 (anatase). No reflections corresponding to vanadium or tungsten crystalline phases were observed. Vanadium oxide crystalline phase reflections are expected at $2\Theta=20.15^{o}$, 26.10^{o} and 31.06^{o} and for tungsten oxide at $2\Theta=24^{o}$ and28^{o}.[58] Casagrande et al. [Casagrande et al. 1999] reported that the absence of appropriate reflections proved the presence of V and W oxides in either an amorphous form or as small crystallites (under 4 nm in diameter). This was also confirmed by Patluru et al. [Patluru et al. 2012] who observed that for concentration of V_2O_5 typical for industrial applications no

complete monolayer is formed, and thus XRD reflections do not appear. No change in the support itself proves that even after twelve months of exposure the transformation of anatase to rutile did not take place.

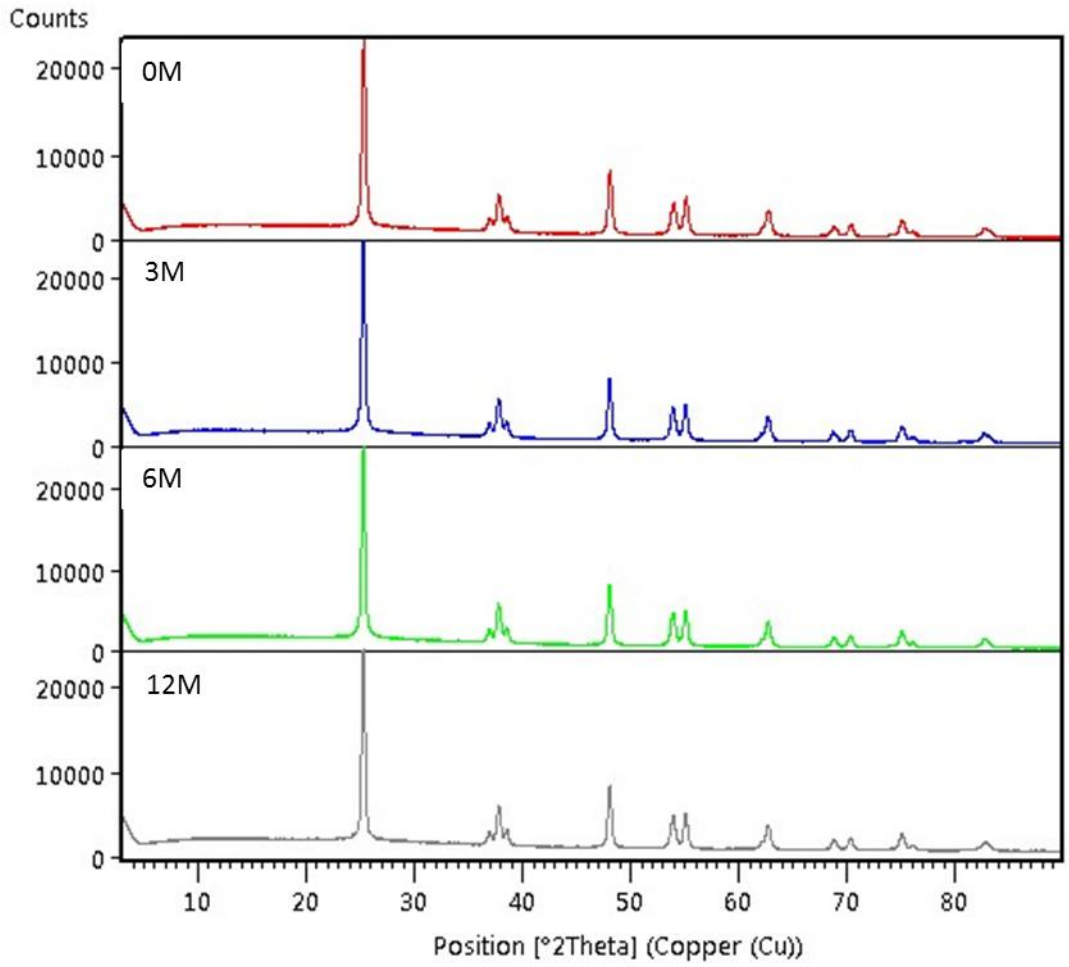

Figure 26 XRD of the studied catalyst

XRD analysis was also performed for all ash samples. The XRD patterns are shown in Figure 27, Figure 28 and Figure 29 and the compounds which were looked for are listed in Table 19. These compounds were selected basing on typical literature findings for different types of fly ash from coal and biomass fired power plants [63, 64], The following crystalline compounds were identified in all ash samples: anhydrite ($CaSO_4$), quartz (SiO_2), sillimunite and mullite. Periclase and magnesium ferrite were observed in 6M. The small amounts of the latter and minor amounts of corundum, andradite and gelehnite are also possible in other ash samples. No TiO_2 was found in any of ash samples.

XRD patterns did not reveal the presence of any potassium compounds either in fly ash or on the catalysts, despite the presence of K in the fly ash, as shown by AAS results. The possible

mechanism of potassium transfer from biomass to fly ash was proposed by Sahu et. al. [2014]. A part of potassium considered as inherent ash vaporizes during combustion. When temperature is getting below condensation, K vapours may be deposited on solid fly ash particles creating potassium sulphates of chlorides.

The absence of potassium compounds in XRD patterns of fly ash or catalysts may be due to the amorphous state of such compounds, or very small crystallites (under detection level). The distribution in the form of very small entities may have been caused by an increased mobility of the K compounds at the temperature of catalyst operation in the power plant (420^{o}C). Nanocrystallites of expected K and Na compounds (NaCl,Na_2SO_4, K_2SO_4 and KCl) might start to melt or sinter creating amorphous islands/layer on the surface of fly ash and/or catalysts due to fairly low Tammann temperature of the considered species, as can be seen in Table 20. From Table 20 it may be concluded that only $CaSO_4$ may be expected in the form of crystallites at 420^{o}C and actually anhydrite was observed in fly ash, as proven by Table 19.

Table 19 Compounds present in ash samples

Compound name	3M ash	6M ash	12M ash
$CaSO_4$ anhydrite	+	+	+
SiO_2 quartz	+	+	+
Mullite	+	+	+
Corundum	-	+ -	-
Andradite	-	+ -	-
Sillimanite	+	+	+
Anorthite	-	-	-
Cristobalite	-	-	-
Gehlenite	-	+ -	-
Periclase	-	+	-
Magnesium ferrite	+ -	+	+ -
TiO_2	-	-	-
K_2SO_4	-	-	-
KCl	-	-	-

Table 20 Melting and Tammann temperatures of K, Na and Ca compounds

	Tt[C]	Ttamm[C]
KCl	770	249
K2SO4	1067	397
CaSO4	1460	594
NaCl	801	264
Na2SO4	884	306

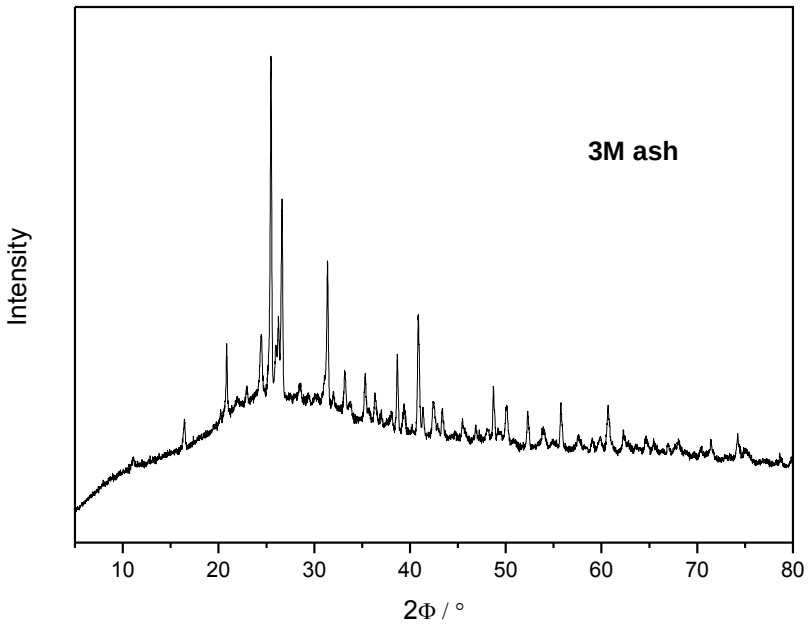

Figure 27 XRD of the 3M ash

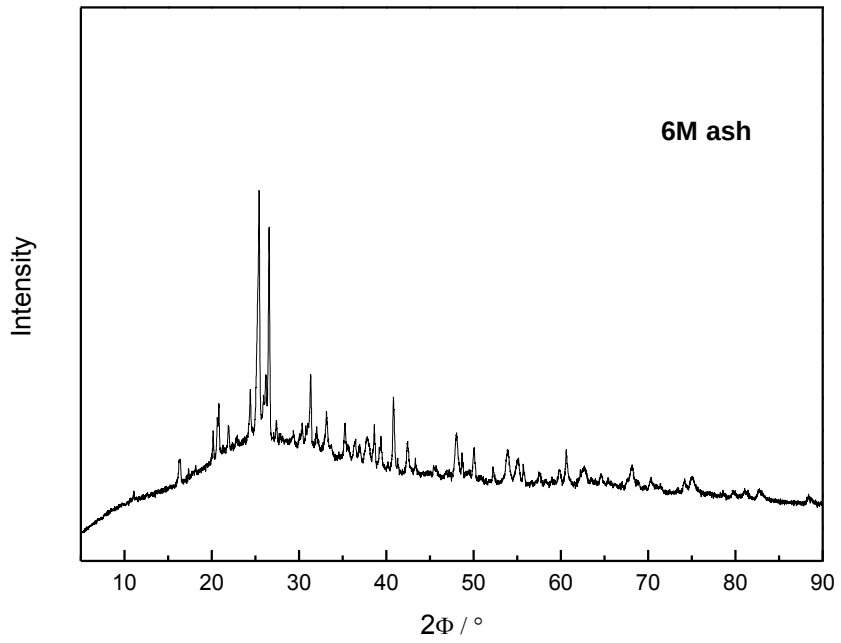

Figure 28 XRD of the 6M ash

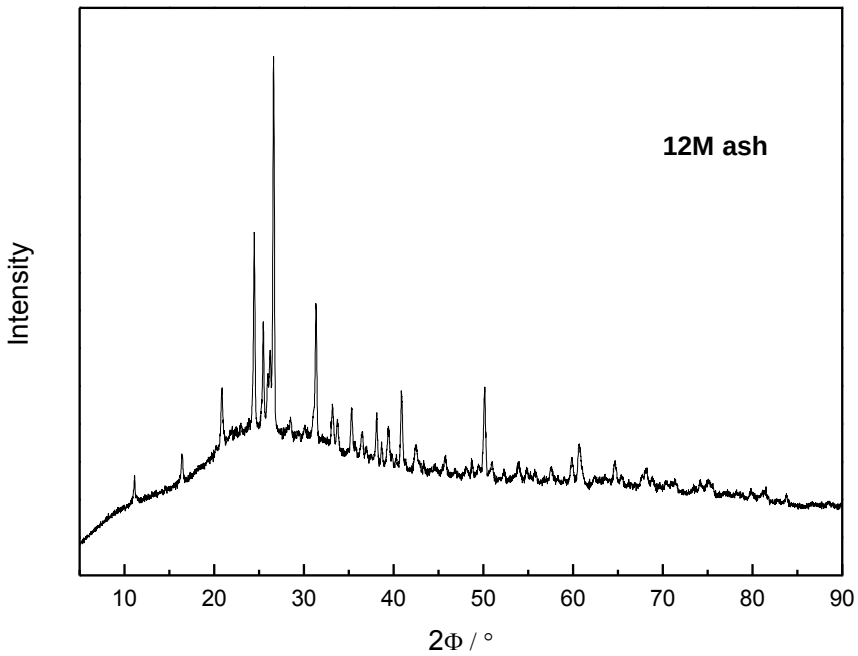

Figure 29 XRD of the 12M ash

5.5 UV-vis

The diffuse reflectance UV–VIS spectra measurement was performed on fresh, 3M, 6M and 12M catalyst samples. The aim of this test was to identify the possible changes of the active phase that could occur during the exposure in the power plant. The spectra are presented in Figure 30. For each sample there are two absorption bands. The first, with a maximum at ca. 240 nm, is most probably the charge–transfer transition of catalyst support $Ti^{4+} \rightarrow O^{2-}$. Similar results were obtained by Piumetti et al. for mesoporous titania catalyst doped with vanadium [Piumetti et al., 2014, Ciambelli et al. 1995]. The second maximum is located at ca. 320 nm and it represents vanadium species. More detailed description of this band was proposed by Satsuma et al. [Satsuma et al. 2002], who interpreted it as charge transfer of O^{2-} to V^{5+} in tetrahedral species. A similar explanation was given by Bourikas et al.[Bouricas et al. 2004]. There are no further bands over 375 nm, which means that neither the fresh catalyst nor the deactivated samples have either polymeric vanadium oxide structures or V^{3+} or V^{4+} species. It must be mentioned, however, that the latter bands were observed in some other studies of vanadium catalysts [Baran et al. 2013][Youn et al. 2014].

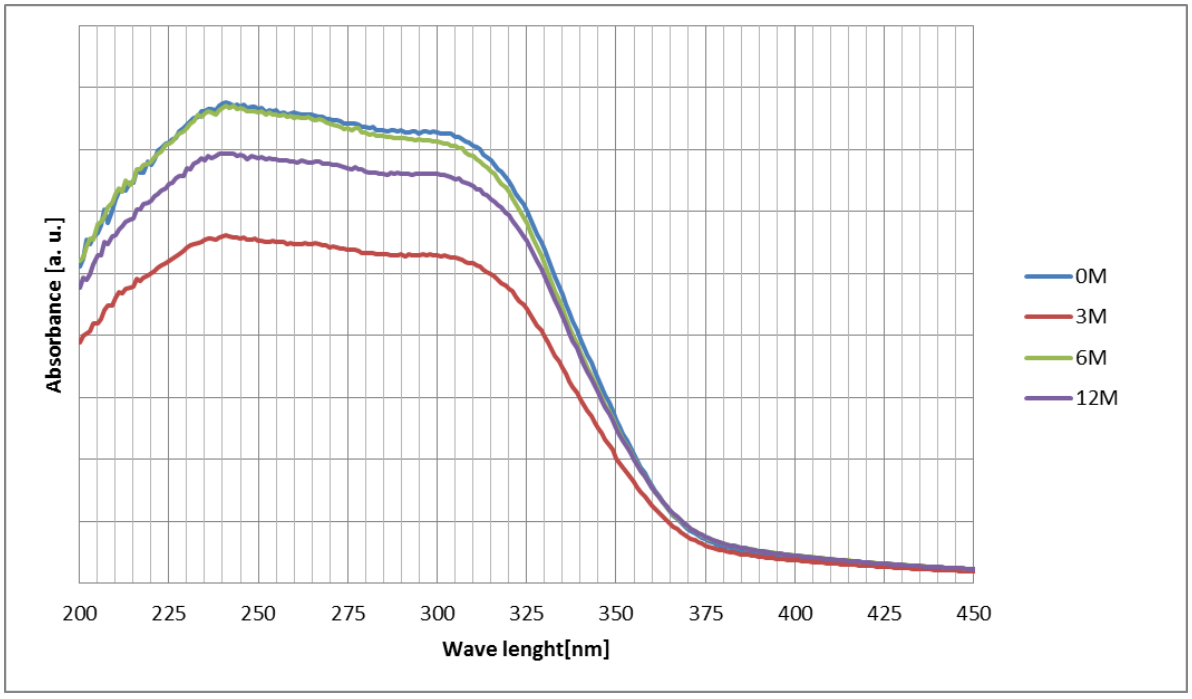

Figure 30 UV-Vis spectra of fresh, 3M, 6M and 12M sample

All examined samples show the same positions of the above discussed bands. No tungsten species are visible in the obtained spectra. The absence of any band shifts in comparison to the fresh

catalyst allows to assume, that neither titanium support nor active vanadium phase were changed during the exposure under industrial conditions of biomass co-fired coal power plant. The only observed difference was the change in total intensity of the observed bands.

5.6 FTIR

FTIR spectra are presented in Figure 31, Figure 32 and Figure 33. In the region of 3900-3500 cm^{-1} (Figure 31) there are several bands, which are connected with OH vibrations. Bands at 3615cm^{-1} were identified in literature [Baran et al. 2013] as vibration of V-OH group. This confirms previous assumptions about existence of V-OH active sites in the studied catalysts although they are slightly shifted to higher wavenumber. The intensity of these peaks can indicate the number of such vanadium species present on catalyst surface [Baran et al. 2013]. It can be observed that with the increasing operation time the peaks became less intense. A possible explanation could be the poisoning with potassium compounds increasing with the increased duration of exposure.

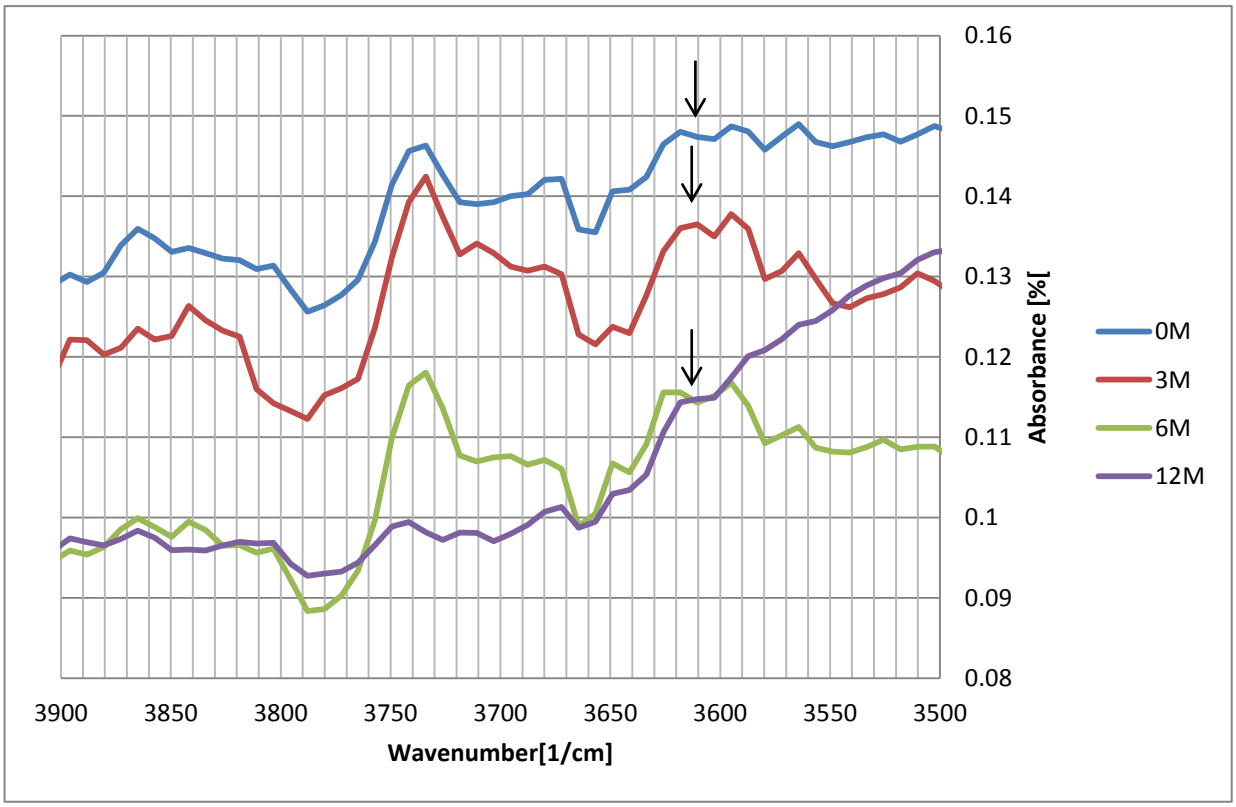

Figure 31 FTIR spectra of tested catalyst samples

The second group of peaks is presented in Figure 32. The band at 1035 cm^{-1} has been identified as stretching vibration of V=O groups [Magg et al. 2004]. These species are believed to take important part in the DeNOx reaction mechanism, together with hydroxide vanadium groups. Similar results were obtained by Piumetti et al. while examining vanadium based catalysts for oxidation reactions [Piumetti et al. 2012]. Also Alemany et al came to identical conclusion while comparing commercial-like V_2O_5-WO_3/TiO_2 $DeNO_x$ catalysts reactivity in SCR reaction [Alemany et al, 2006]. For the studied samples: fresh, 3M and 6M this peak has a comparable intensity. It allows to assume, that the number of V=O sites during operation time did not change significantly, in contrast to V-OH groups poisoned by alkali metals. Higher absorption observed for sample 12M may arise from the aggregation of the vanadyl species into bigger clusters. An alternative explanation could be the superposition of the discussed band with the band at 1043 cm^{-1} interpreted as the vibrations of monomeric sulphate species bound bidentate to anatase [Kristensen et al, 2011]. As pointed by Kristensen et al, the FTIR spectra of catalysts treated with H_2SO_4 showed new peaks at 1215, 1135 and 1043 cm^{-1}.The wide peak below 800 cm^{-1} (Figure 33) may be interpreted as TiO_2 in the form of anatase in good agreement with Alemeny et al [Alemany et al. 1995].It is similar for all samples, which supports UV-VIS results of the lack of the changes in titanium support having occurred during the exposure in the power plant.

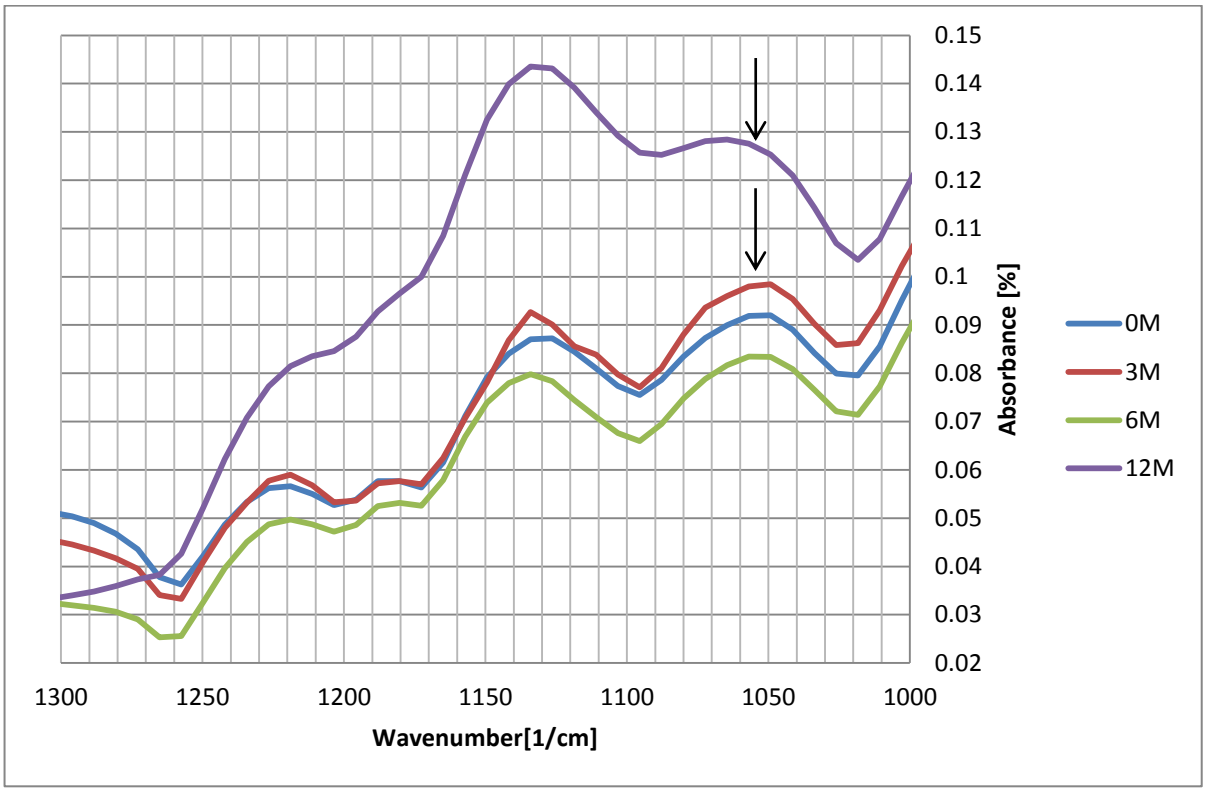

Figure 32 FTIR spectra of tested catalyst samples

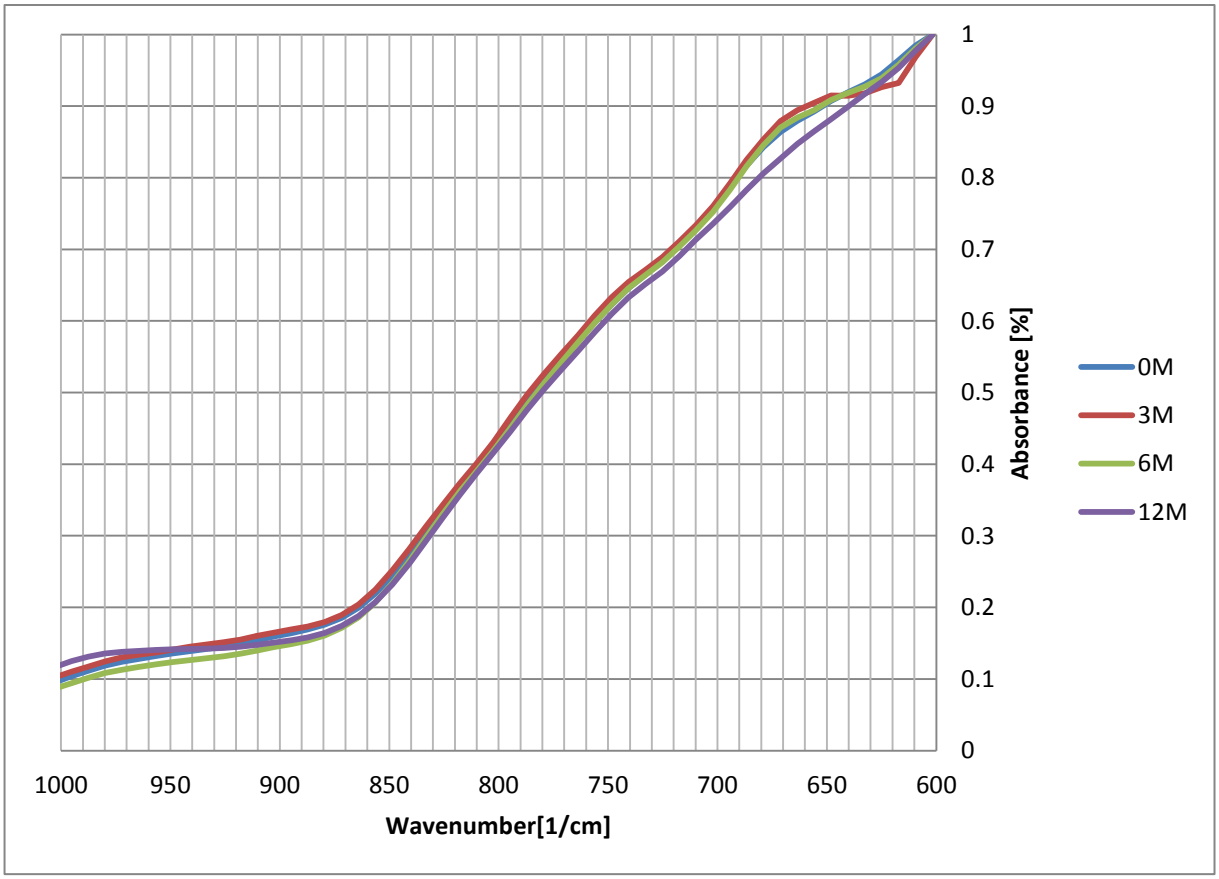

Figure 33 FTIR spectra of tested samples

5.7 Butene isomerization

The purpose of this measurement was to check how the exposure to real flue gas influenced the acidity of the commercial catalyst. Figure 34 shows conversion of 1-butene as a function of temperature.

For the fresh catalyst the reaction rate increased with the rising temperature almost linearly from 20% to 60% at 250^{o}C. For all catalysts after the exposure to flue gas, the dependence of conversion on temperature differed from that for the fresh catalyst, indicating a different type of acidic sites.

Surprisingly high conversion was obtained for the catalyst after three months of exposure. The explanation may be connected with the fact that the catalyst bed was installed in the high-dust configuration, and thus apart from the influence of ash, also the interaction with SO_2 and SO_3 must be taken into account. These additional acid sites which raised the conversion of 1-butene to 2-butene for 3M catalyst most probably arise from the formation of surface sulphate (VI) species. Li et al [Li et al

2015] studied the combined effect of KCl and SO_2 on SCR catalysts and concluded from TPAD and FTIR experiments that although acidity was increased by the deposition of sulphate groups, the activity test in the presence of SO_2 had little effect on ammonia adsorption. This would suggest that these groups did not take part directly in SCR reaction. This is in good agreement with the results of the presented MSc thesis – although acidity increased, deactivation (arising from the deposition of alkalis) was observed. The discussed sulphate groups may have, however, influenced the extent of poisoning by K^+. Putluru et al. [Putluru et al, 2012] suggested that sulphation of the support would be beneficial because alkali species would interact stronger with such support than with the active sites (vanadium).

Following the above explanation, initial SO_x concentration on surface could be considered as beneficial for the 3M catalyst, while for 6M and 12 M the effect of deactivation by the increasing deposition of alkalis prevailed, leading to the poisoning of additional acidic sites of vanadium. This confirms the studies concerning potassium poisoning of –V-OH species [Kristensen et al. 2011][Chen et al. 2010]

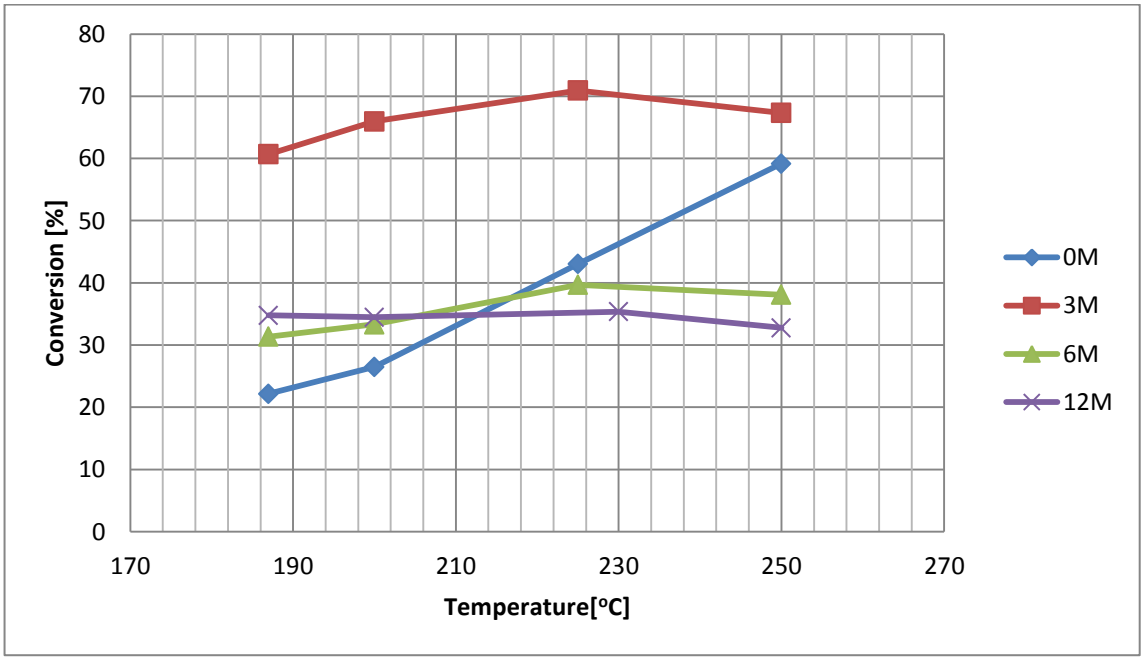

Figure 34 Conversion of 1-butene to 2-butene as a function of temperature

6. Conclusions

The aim of this work was to investigate the influence of biomass addition to fuel on SCR catalyst. What differed this study from many other DeNOx catalyst investigations, was the examined samples. Thanks to cooperation with EDF Polska, there was an opportunity to examine commercial honeycomb SCR catalyst deactivated under industrial conditions in the full scale coal-fired boiler. EDF Polska provided the data about the biomass type and share, as well as about conversion of NO for both fresh and exposed catalysts, allowing the conclusions concerning the extent of deactivation. In the presented MSc thesis, fresh and deactivated catalysts were characterized and compared to the data from literature obtained in the laboratory-scale studies. The fresh and deactivated catalysts, as well as ash collected on the catalysts during their exposure to flue gas in the power plant, were characterized by atomic absorption spectrometry AAS, scanning electron microscopy SEM and EDS, X-ray diffraction XRD, UV-VIS spectroscopy and infrared spectroscopy HATR. The acidity of the studied samples was determined with the aid of the model reaction – isomerisation of 1-butene to 2-butene.

From the performed experiments, the following conclusions may be drawn:

- Atomic absorption spectroscopy results had confirmed the presence of potassium in ash samples, much higher than in ash coming from coal combustion alone, as well as the concentration of K in the studied catalyst samples increasing with the time of exposure. The elevated potassium concentration found in the catalyst most probably originated from the co-fired biomass.

- The EDS analysis partially confirmed these results, and revealed potassium in both ash and the catalyst after 9405h exposure (12M sample). Additionally, a relatively high concentration of sulphur was observed in the catalyst samples, increasing after exposure in comparison to the fresh catalyst. The comparison of K and S allows the conclusion, that apart from K_2SO_4, also other S-containing species were formed on the catalysts.

- The X-ray patterns of catalyst samples showed that the support TiO_2 (anatase) did not change during exposure. On the other hand, no vanadium compounds were registered, which points either to very small crystallites or amorphous structure. XRD of ash samples showed Si, Ca, Al compounds, typically found in coal ash, with no clear presence of potassium compounds.

- UV-Vis study was performed to determine more specifically what kind of vanadium oxides can be found on catalyst surface. The results showed the presence of tetrahedral V^{5+} species, with no signs of either V^{4+}, V^{3+} or polymeric vanadium oxides. Ti^{4+} species were also registered.

- The decreasing trend in V-OH groups concentration was observed in the FT-IR measurement, confirming the statements found in literature, that potassium cations substituted hydrogen in these groups, excluding them from SCR reaction.

- Butene conversion measurements revealed the increase in acidity for shorter times of exposure (2270h) and the following decrease in acidity for the longer times (4527h and 9405h), despite the decrease in NOx conversion for all mentioned samples. The possible explanation may be connected with the formation of sulfate groups which are acidic in character. They do not form, however, the sites for DeNOx reaction. Still they may play a positive role and decrease the rate of deactivation during the first periods of exposure, forming the sites for potassium cations adsorption and thus protecting V-OH DeNOx reaction sites.

The information obtained for the catalysts exposed to flue gas under industrial conditions, may influence the choice of biomass and possibly influence the future strategy for the commercial catalysts regeneration. Some additional data, however, will be needed, especially the surface composition. The regeneration processes could be similar to those suggested in literature, e.g. washing with aqueous solutions of certain acids, to remove K^+ cations from the surface.

Bibliography

LUIS J. ALEMANY, LUCA LIETTI, NATALE FERLAZZO, PIO PORZATTI, GUIDO BUSCA, ELIO GIAMELLO, FIORENZO BREGANI, “Reactivity and Physicochemical Characterisation of V_2O_5-WO_3/TiO_2 $DeNO_x$ Catalysts”, Journal of Catalysis vol. 155, p. 117-130, 1995

KALYAN ANNAMALAI, ISHWAR K. PURI, “Combustion science and ingeneering” 2007, p. 771-773

RAFAŁ BARAN, THOMAS ONFROY, TERESA GRZYBEK, STANISŁAW DZWIGAJ, “Influence of the nature and environment of vanadium in VSiBEA zeolite on selective catalytic reduction of NO with ammonia”, Applied Catalysis B: Environmental vol. 136-137, p. 186-192, 2013

K. BOURIKAS, CH. FOUNTZOULA, CH. KORDULIS, “Monolayer transition metal supported on titania catalysts for the selective catalytic reduction of NO by NH_3”, Applied Catalysis B: Environmental vol. 52, p. 145-153, 2004

ELŻBIETA BULEWICZ, ARKADIUSZ DYJAKON, TOMASZ HARDY, WŁODZIMIERZ KORDYLEWSKI, STANISŁAW SŁUPEK, RYSZARD MILLER, ADAM WANIK, „Spalanie i paliwa” 2005

GUIDO BUSCA, LUCA LIETTI, GIANGUIDO RAMIS, FRANCESCO BERTI, “Chemical and mechanistic aspects of the selective catalytic reduction of NOx by ammonia over oxide catalysts: A review”, Applied Catalysis B: Environmental vol. 18, p. 1-36, 1998

LAURA CASAGRANDE, LUCA LIETTI, ISABELLA NOVA, PIO FORZATTI, ALFONS BAIKER, “SCR of NO by NH3 over TiO2-supported V2O5–MoO3 catalysts: reactivity and redox behavior” Applied Catalysis B: Environmental vol. 22, p. 63-77, 1999

MARZIA CASANOVA, ELIANA ROCCHINI, ALESSANDRO TROVARELLI, KARL SCHERMANZ, IRENE BEGSTEIGER, “High-temperature stability of V2O5/TiO2-WO3-SiO2 SCR catalysts modified with rare-earths” Journal of Alloys and Compounds 408-412, p. 1108-1112, 2005

MARZIA CASANOVA, KARL SCHERMANZ, JORDI LLORCA, ALESSANDRO TROVARELLI, “Improved high temperature stability of NH3-SCR catalysts based on rare earth vanadates supported on TiO2 WO3 SiO2” Catalysis Today vol. 184, p. 227-236, 2012

FRANCESCO CASTELLINO, SØREN BIRK RASMUSSEN, ANKER DEGN JENSEN, JAN ERIK JOHNSSON, RASMUS FEHRMANN, “Deactivation of vanadia-based commercial SCR catalysts by polyphosphoric acids”, Apllied Catalysis B: Environmental vol. 83, p. 110-122, 2008

LANG CHEN, JIN ZHAO, SHUANG-FENG YIN, CHAK-TONG AU, “A mini-review on solid superbase catalysts developed in the past two decades” 2012

LIANG CHEN, JUNHUA LI, MAOFA GE," The poisoning effect of alkali metals doping over nano V2O5–WO3/TiO2 catalysts on selective catalytic reduction of NOx by NH3" Chemical Engineering Journal vol. 170, p. 531-537, 2010

PAOLO CIAMBELLI, LUCIANA LISI, GENNARO RUSSO, JEAN CLAUDE VOLTA, "Physico-chemical study of selective catalytic reduction vanadia-titania catalysts prepared by the equilibrium adsorption method", Applied Catalysis B: Environmental vol. 7, p.1-18, 1995

JOHANNES DUE-HANSEN, SOGHOMON BOGHOSIAN, ARKADY KUSTO, PETER FRISTRUP, GEORGE TSILOMELEKIS, KENNY STÅHL, CLAUS HVIID CHRISTENSEN, RASMUS FEHRMANN, "Vanadia-based SCR catalysts supported on tungstated and sulfated zirconia: Influence of doping with potassium", Journal of Catalysis vol. 251, p. 459-473, 2007

EUROPEAN COMMISSION, "Integrated Pollution Prevention and Control:Reference Document on Best Available Techniques for Large Combustion Plants", 2006

EUROPEAN PARLAMENT, "Directive 2010/75/UE about emissions in industry", 2010

P. FORZATTI, "Present status and perspectives in de-NOx SCR catalysis", Applied Catalysis A: General vol. 222, p. 221-236, 2001

R. GARCÍA, A. P. BÁEZ, "Atomic Absorption Spectrometry (AAS)" InTech, 2012

TERESA GRZYBEK, JERZY KLINIK, BARBARA DUTKA, HELMUT PAPP, VLADIMIR SUPRUN, "Reduction of N_2O over carbon fibers promoted with transition metal oxides/hydroxides", Catalysis Today vol. 101, p. 93–107, 2005

TERESA GRZYBEK, MARIA ROGÓŻ, HELMUT PAPP, "The interaction of NO with active carbons promoted with transition metal oxides/hydroxides" Catalysis Today vol. 90, p. 61-68, 2004

BOB HAFNER, "Energy Dispersive Spectroscopy on the SEM: A Primer" University of Minnesota-Twin Cities, 2007

RONALD M. HECK, ROBERT J. FARRAUTO, "Catalytic Air Pollution Control" 1995

HITACHI, "Comparison of Plate Type Catalyst With Honeycomb and Corrugated Catalyst For Ash-Pluggage Potential" 2012

SEONG MOON JUNG, PAUL GRANGE, "Characterization and reactivity of V_2O_5-WO_3 supported on TiO_2-SO_4^{2-} catalyst for the SCR reaction" Applied Catalysis B: Environmental vol. 32, p. 123-131, 2000

HIROYUKI KAMATA, KATSUMI TAKAHASHI, C.U. INGEMAR ODENBRAND, "The role of K_2O in the selective reduction of NO with NH_3 over a V_2O_5 (WO_3)/TiO_2 commercial selective catalytic reduction catalyst" Journal of Molecular Catalysis A: Chemical vol. 139, p. 189-198, 1998

M. KLIMCZAK, P. KERN, T. HEINZELMANN, M. LUCAS, P. CLAUS, “High-throughput study of the effects of inorganic additives and poisons on NH3-SCR catalysts—Part I: V2O5–WO3/TiO2 catalysts” Applied Catalysis B: Environmental vol. 95, p.39-47, 2009

MOTONOBU KOBAYASHI, KATSUNORI MIYOSHI, “WO3–TiO2 monolithic catalysts for high temperature SCR of NO by NH3: Influence of preparation method on structural and physico-chemical properties, activity and durability” Applied Catalysis B: Environmental vol. 72, p. 253-261, 2006

PATRICK G.W.A. KOMPIO, ANGELIKA BRÜCKNER, FRANK HIPLER, GERHARD AUER, ELKE LÖFFLER, WOLFGANG GRÜNERT, “A new view on the relations between tungsten and vanadium in V2O5AWO3/TiO2 catalysts for the selective reduction of NO with NH3” Journal of Catalysis vol. 286, p. 237-247, 2011

WŁODZIMIERZ KORDYLEWSKI, TOMASZ HARDY, “Niskoemisyjne techniki spalania: problemy i perspektywy” 2000

NIKOLAOS KOUKOUZA, JOUNI HÄMÄLÄINEN, DIMITRA PAPANIKOLAOU, ANTTI TOURUNEN, TIMO JANTTI, “Mineralogical and elemental composition of fly ash from pilot scale fluidised bed combustion of lignite, bituminous coal, wood chips and their blends”, Fuel vol. 86, p. 2186-2193, 2007

STEFFEN B. KRISTENSEN, ANDREAS J. KUNOV-KRUSE, ANDERS RIISAGER, SØREN B. RASMUSSEN, RASMUS FEHRMANN, “High performance vanadia–anatase nanoparticle catalysts for the Selective Catalytic Reduction of NO by ammonia” Journal of Catalysis vol. 284, p. 60-67, 2011

KUCOWSKI J., LAUDYN D., PRZEKWAS M., „Energetyka a ochrona środowiska” 1993

JÓZEF KUROPKA, „Oczyszczanie gazów odlotowych z zanieczyszczeń gazowych: Urządzenia i technologie” 1991

ANN-CHARLOTTE LARSSON, JESSICA EINVALL, ARNE ANDERSSON, AND MEHRI SANATI, “Physical and chemical characterisation of potassium deactivation of a SCR catalyst for biomass combustion” Topics in Catalysis vol. 45, p. 149-152, 2007

JUNHUA LI, HUAZHEN CHANGA, LEI MAA, JIMING HAOA, RALPH T. YANG, “Low-temperature selective catalytic reduction of NOx with NH3 over metal oxide and zeolite catalysts—A review” Catalysis Today vol. 175, p. 147-156, 2011

QICHAO LI, SIFAN CHEN, ZHENYU LIU, QINGYA LIU, “Combined effect of KCl and SO_2 on the selective catalytic reduction of NO by NH3over V_2O_5/TiO_2 catalyst” Applied Catalysis B: Environmental vol.164, p. 475-482, 2015

ZHIMING LIU, JUNHUA LI, ABU S.M. JUNAIDC, “Knowledge and know-how in improving the sulfur tolerance of deNOx catalysts” Catalysis Today vol. 153, p. 95-102, 2010

NORBERT MAGG, BOONCHUAN IMMARAPORN, JAVIER B. GIORGI, THOMAS SCHROEDER, MARCUS BÄUMER, JENS DÖBLER, ZILI WU, EVGENII KONDRATENKO, MAYMOL CHERIAN, MANFRED BAERNS, PETER C. STAIR, JOACHIM SAUER, HANS-JOACHIM FREUND, “Vibrational spectra of alumina- and silica-supported vanadia revisited: An experimental and theoretical model catalyst study”, Journal of Catalysis vol. 226, p. 88-100, 2004

BRUCE MILLER, DAVID TILLMAN, „Combustion engineering issues for solid fuel systems” 2008

D. NICOSIA, I. CZEKAJ, O. KRÖCHER, „Chemical deactivation of V2O5/WO3–TiO2 SCR catalysts by additives and impurities from fuels, lubrication oils and urea solution Part II. Characterization study of the effect of alkali and alkaline earth metals” Applied Catalysis B: Environmental vol. 77, p. 228-236, 2007

J. W. NIEMANTSVERDRIET, “Spectroscopy in catalysis, 2nd edition”, 2000

ISABELLA NOVA, LORENZO DALL’ACQUA, LUCA LIETTI, ELIO GIAMELLO, PIO FORZATTI, “Study of thermal deactivation of a de-NOx commercial catalyst” Applied Catalysis B: Environmental vol. 35, p. 31-42, 2001

F. PADERA, “UV/Vis Spectroscopy”, PerkinElmer, Shelton 2013

DONOVAN A. PEÑA, BALU S. UPHADE, PANAGIOTIS G. SMIRNIOTIS, “TiO2-supported metal oxide catalysts for low-temperature selective catalytic reduction of NO with NH3: I. Evaluation and characterization of first row transition metals”, Journal of Catalysis vol. 221, p. 421-431, 2003

MARCO PIUMETTI, EDOARDO GARRONE, FABRIZIO CAVANI, ILENIA ROSSETTI, BARBARA BONELLI, “Vanadium-containing catalysts for oxidation reactions”, Catalysis Applications vol. 30, p. 29-34, 2012

MARCO PIUMETTI, FRANCESCA STEFANIA FREYRIAA, MARCO ARMANDIA, FRANCESCO GEOBALDOA, EDOARDO GARRONEA, BARBARA BONELLIA, “Fe- and V-doped mesoporous titania prepared by direct synthesis: Characterization and role in the oxidation of AO7 by H_2O_2 in the dark”, Catalysis Today vol. 227, p. 71-79, 2014

SIVA SANKAR REDDY PUTLURU, STEFFEN BUUS KRISTENSEN, JOHANNES DUE-HANSEN, ANDERS RIISAGER, RASMUS FEHRMANN, “Alternative alkali resistant deNOx catalysts”, Catalysis Today vol. 184, p. 192-196, 2012

S. J. B. REED, “Electron microprobe analysis and scanning electron microscopy in geology” 2005

M. RICHTER, A. TRUNSCHKE, U. BENTRUP, K.-W. BRZEZINKA, E. SCHREIER, M. SCHNEIDER, M.-M. POHL, R. FRICKE, “Selective Catalytic Reduction of Nitric Oxide by

Ammonia over Egg-Shell MnOx/NaY Composite Catalysts", Journal of Catalysis vol. 206, p. 98-113, 2002

ROYAL SOCIETY OF CHEMISTRY, "Atomic absorption spectrometry" 2000

MARIA PIA RUGGERIA, ANTONIO GROSSALEA, ISABELLA NOVA, ENRICO TRONCONIA, HANA JIRGLOVA, ZDENEK SOBALIK, "FTIR in situ mechanistic study of the NH3 NO/NO2 "Fast SCR" reaction over a commercial Fe-ZSM-5 catalyst" Catalysis Today vol. 184, 107-114, 2011

S.G. SAHU, N.CHAKRABORTY, P.SARKAR, "Coal–biomass co-combustion: An overview", Renewable and Sustainable Energy Reviews vol. 39, p. 575-586, 2014

ATSUSHI SATSUMA, SAKAE TAKENAKA, TSUNEHIRO TANAKA, SHIGERU NOJIMA, YOSHIYA KERA, HISASHI MIYATA, "Studies on the preparation of supported metal oxide catalysts using JRC-reference catalysts II. Vanadia–titania catalyst: effect of starting solution and phase of titania", Apllied Catalysis A: General vol. 232, p. 93-106, 2002

T. SCHWÄMMLE, F.BERTSCHE, A.HARTUNG, J.BRANDENSTEIN, B.HEIDEL, G.SCHEFFKNECHT, "Influence of geometrical parameters of honeycomb commercial SCR-DeNOx-catalysts on DeNOx-activity, mercury oxidation and SO2/SO3-conversion" Chemical Engineering Journal vol. 222, p. 274-281, 2013

GON SEO, HWAN SEOK JEONG, SUK BONG HONG AND YOUNG SUN UH, "Skeletal isomerization of 1-butene over ferrierite and ZSM-5 zeolites: influence of zeolite acidity" Catalysis Letters vol. 36, p. 249-253, 1995

O. SIMON, "EXPLOITATION EXPERIENCES WITH CONVENTIONAL FLUEGAS CLEANING SYSTEMS" Radiat. Phys. Chem. vol. 45, p. 1057-1062, 1995

JOSHUA R. STREGE, CHRISTOPHER J. ZYGARLICKE, BRUCE C. FOLKEDAHL, DONALD P. MCCOLLOR, "SCR deactivation in a full-scale cofired utility boiler" Fuel vol. 87, p. 1341-1347, 2007

THERMO NICOLET CORPORATION, "Introduction to Fourier Transform Infrared Spectrometry" 2001

D.A. TILLMAN, "Biomass cofiring: the technology, the experience, the combustion consequences", Biomass and Bioenergy vol. 19, p. 364-384, 2000

VESNA TOMASIC, "Application of the monoliths in DeNOx catalysis" Catalysis Today vol. 119, p. 106-113, 2006

SANDER VAN DONK, JOHANNES H. BITTER, KRIJN P. DE JONG, "Deactivation of solid acid catalysts for butene skeletal isomerisation: on the beneficial and harmful effects of carbonaceous deposits" Applied Catalysis A: General vol. 212, p. 97-116, 2001

MARIA ANGELES LARRUBIA VARGAS, MARZIA CASANOVA, ALESSANDRO TROVARELLI, GUIDO BUSCA, “An IR study of thermally stable V2O5-WO3 -TiO2 SCR catalysts modified with silica and rare-earths (Ce, Tb, Er)” Applied Catalysis B: Environmental vol. 75, p. 303-311, 2007

ISRAEL E. WACHS, BERT M. WECKHUYSEN, “Structure and reactivity of surface vanadium oxide species on oxide supports” Applied Catalysis A: General vol. 157, p. 67-90, 1997

B. E. WARREN, “X-Ray diffraction”, Dover Publications, New York 1990

KATE WIECK-HANSENA, PETER OVERGAARD, OLE HEDE LARSEN, “Cofiring coal and straw in a 150MWe power boiler experiences”, Biomass and bioenergy vol. 19, p. 395-409, 2000

R. WILLI, B. RODUIT, R.A. KOEPPEL, A. WOKAUN, A. BAIKER, “Selective reduction of no by nh3 over vanadia-based commercial, catalyst: parametric sensitivity and kinetic modeling” Chemical Engineering Science vol. 51, p. 2897-2902, 1996

JIMMIE L. WILLIAMS, “Monolith structures, materials, properties and uses”, Catalysis Today vol. 69, p. 3-9, 2001

www.mitsui-mining.co.jp/index2.html

YU YAN-KE, HE CHI, CHEN JIN-SHENG, MENG XIAO-RAN, “Deactivation mechanism of de-NOx catalyst (V2O5-WO3/TiO2) used in coal fired power plant” Journal of Fuel Chemistry And Technology vol. 40, p. 1359-1365, 2012

SEUNGHEE YOUN, SOYEON JEONG, DO HEUI KIM, “Effect of oxidation states of vanadium precursor solution in V_2O_5/TiO_2catalysts for low temperature NH_3 selective catalytic reduction”, Catalysis Today vol. 232, p. 185-191, 2014

WILLIAM H. ZACHARIASEN, “Theory of X-Ray diffraction in crystals”, Dover Publications, New York, 1967

SHULE ZHANG, QIN ZHONG, “Promotional effect of WO3 on O2− over V2O5/TiO2 catalyst for selective catalytic reduction of NO with NH3” Journal of Molecular Catalysis A: Chemical vol. 373, p. 108-113, 2013

YUANJING ZHENG, ANKER DEGN JENSEN, JAN ERIK JOHNSSON, “Deactivation of V2O5-WO3-TiO2 SCR catalyst at a biomass-fired combined heat and power plant” Applied Catalysis B: Environmental vol. 60, p. 253-264, 2005